2016

The comparison of Friedel-Crafts alkylation and acylation as a means to synthesise alkyl xylenes

Whalley, P.

Whalley, P. (2016) 'The comparison of Friedel-Crafts alkylation and acylation as a means to synthesise alkyl xylenes', The Plymouth Student Scientist, 9(1), p. 252-296.
http://hdl.handle.net/10026.1/14124

The Plymouth Student Scientist
University of Plymouth

*The Plymouth Student Scientist, 2016, **9**, (1), 252-296*

The comparison of Friedel-Crafts alkylation and acylation as a means to synthesise alkyl xylenes

Penny Whalley

Project Advisor: Anthony Lewis, School of Geography, Earth and Environmental Sciences, Plymouth University, Drake Circus, Plymouth, PL4 8AA

Abstract

The aim of this project was to synthesise and characterise an alkyl xylene using both a Friedel-Crafts alkylation and a Friedel-Crafts acylation. The literature stated that whilst alkylation raised many issues with polyalkylation, transalkylation, dealkylation and rearrangement of the electrophile, acylation with subsequent reduction of the carbonyl provided a far less problematic route. Firstly, Friedel-Crafts alkylation of *m*-xylene was performed using *t*-butyl chloride. The product was purified by vacuum distillation and rotary evaporation. Analysis using IR, GC-FID, GC-MS and NMR allowed the conclusion of a 1,3,5-trisubstituted benzene product. Secondly, Friedel-Crafts acylation of *m*-xylene was performed using butyryl chloride. Analysis using IR, GC-FID, GC-MS and NMR allowed the conclusion of a 1,2,4-trisubstituted benzene product. The product of the alkylation reaction was unexpected due to the pre-existing methyl groups being *ortho-para*-directing. It was concluded that attack at the *ortho* and *para* positions allowed the intermediates to be stabilised, however due to steric hindrance the products would be of higher energy. It was therefore deemed that the acylation reaction product was kinetically controlled as the energy of the intermediates most influenced it; however, the alkylation reaction product was thermodynamically controlled. Literature stated this was likely to do with the reversibility of the alkylation reaction and the irreversibility of the acylation reaction. Grignard reactions were carried out on the synthesised acyl xylene using ethyl bromide and propyl bromide. With both reactions, a new peak at 3500 cm^{-1} occurred on the IR confirming synthesis of an alcohol. GC-MS analysis showed residual acyl xylene in the crude product as well as several peaks displaying the fragmentation patterns for the expected product. It was concluded that the GC-MS for the reaction using ethyl bromide displayed a greater number of peaks with similar fragmentation patterns due to the introduction of a chiral carbon. Further research suggested included the dehydration and hydrogenation of the Grignard products, the acylation and alkylation reactions carried out at varying temperatures and the acylation carried out with a branched acyl chloride.

Introduction

Large varieties of products used in various fields of human activity are based on the processing of aliphatic and aromatic hydrocarbons (Odochian *et al*., 2010). By proper conditions of their transformations on both a small and large scale, aromatic hydrocarbons can be submitted to oxidative and hydrogenation (Juganaru *et al*., 2007) processes as well as electrophilic substitutions, thus synthesising final products and intermediates for multiple other uses (Odochian *et al.*, 2010).

Petroleum is one of the main sources of raw materials for the chemical industry and offers products and by-products suitable for further processing into useful materials (Odochian *et al.*, 2010). One of the components of the petroleum mixture is the xylenes (dimethylbenzenes). Xylenes are important raw materials for the organic synthesis of the nitro musks including xylene musk, ketone musk and thibetin musk (Odochian *et al.*, 2010).

Friedel-Crafts alkylation is a classic electrophilic aromatic substitution often used in the preparation of alkyl-substituted benzene. The Friedel-Crafts reaction is well studied and reported extensively by Olah (Olah, 1963). Due to the nucloephilicity of aromatic compounds being relatively low, extreme conditions for the intermolecular process with alkyl halides are common (Kaneko, Hayashi & Cook, 2007). Typically, the reaction is performed using an alkyl halide for alkylation. The process is conventionally catalysed through the use of Lewis acids such as $AlCl_3$ or BF_3, $ZrCl_4$ and $FeCl_3$ (Wang *et al.*, 2011).

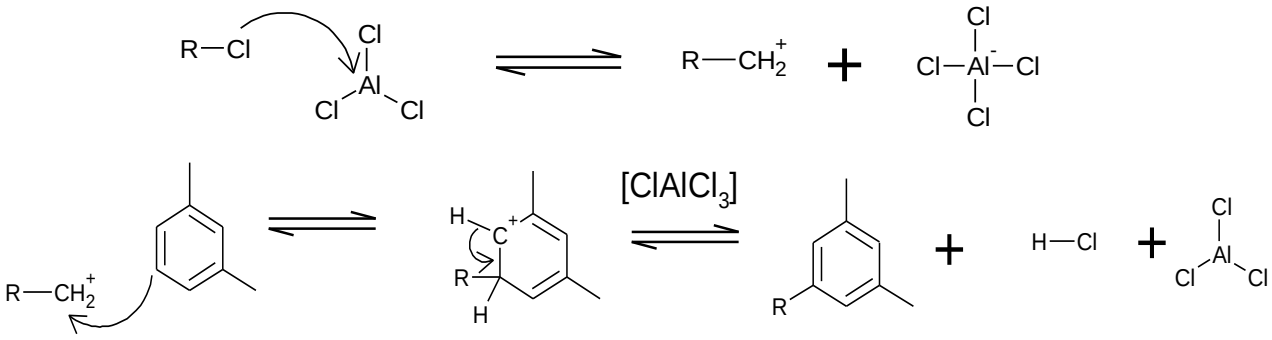

Figure 1: The mechanism of the Friedel-Crafts alkylation of *m*-xylene (March, 1992)

However, with Friedel-Crafts alkylation, several problems can arise. First, the alkyl group is deemed to be activating and increases the reactivity of the aromatic ring, which may lead to polyalkylation. However, the use of simple alkyl groups such as ethyl or isopropyl substituents often allows high yields of monoalkyl products to be obtained, as these are attacked only about 1.5 to 3 times as fast as benzene (Olah, Kuhn & Flood, 1962).

Second, transalkylation or dealkylation can occur which may provide a bigger obstacle. This has been studied in detail in the formation of toluene and/or trimethylbenzenes (Chao & Leu, 1989; Toch *et al*., 2012). Jin *et al*. (2013) also noted it in a paper that *o*-xylene undergoes isomerism in the presence of the $AlCl_3$ catalyst to form the other two isomeric xylenes. This could also be problematic if the methyl groups on *m*-xylene were to undergo similar isomerism.

In contrast, Friedel-Crafts acylation of *m*-xylene could prove to be less problematic concerning the synthesis of a known product. The literature surrounding the mechanistic aspects of electrophilic aromatic substitution reactions is extensive. The mechanism of acylation is largely the same as for alkylation with the use of an acid anhydride or acid chloride as opposed to an alkyl halide.

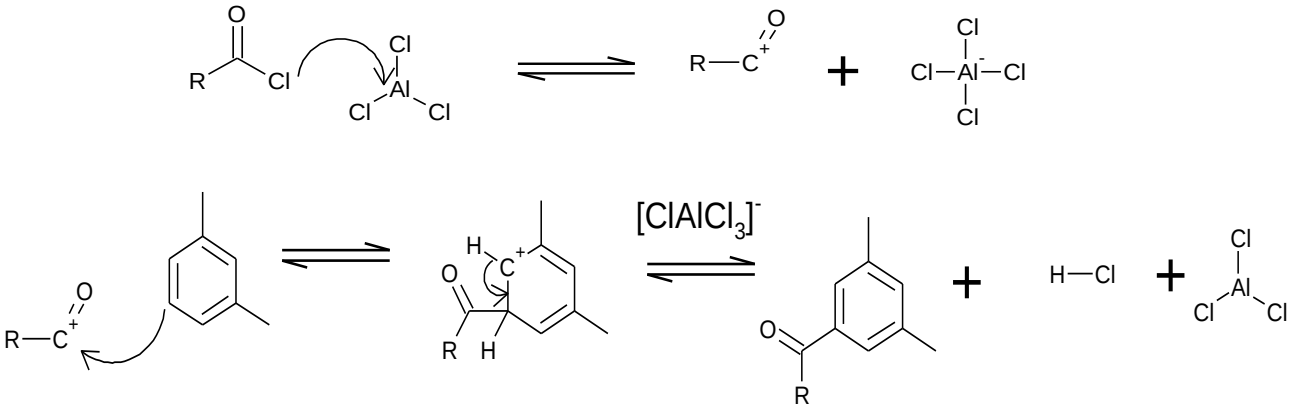

Figure 2: One of the proposed mechanisms for the acylation of *m*-xylene using an acyl chloride (March, 1992)

Acylation of *m*-xylene would not carry the same risk of polyalkylation as the acyl group is deactivating which would cause the ring to become less reactive. Furthermore, the acylium ion is more stable and so rearrangement of the carbocation is less likely (Clayden, Greeves & Warren, 2012).

It is stated in March (1992), that compounds which contain *ortho-para*-directing groups such as the alkyl substituents are acylated easily and yield mainly the para products owing to the large size of the acyl group. This is also confirmed by Odochian *et al.* (2010) with regards to alkylation with *t*-butyl chloride, who states that as the *t*-butyl cation is a bulky electrophile, steric hindrance with the pre-existing methyl groups will cause the reaction to favour the *para* position. With this in mind, it could be assumed that when acylating *m*-xylene the acyl group would in fact attach at the *meta* position as this position offers the least steric hindrance. However, in the alkylation of *m*-xylene with *t*-butyl chloride, Ismail *et al*. (2008), reported the products observed were 1,2,3- and 1,2,4- trisubstituted benzenes, suggesting the product alkylates in both the *ortho* and *para* positions. These findings suggest that perhaps the ortho-para-directing groups have a larger influence over the position of substitution than steric hindrance.

One way to synthesise a known isomer could be using a selective catalyst. Beta-zeolite is known to be an efficient catalyst for Friedel-Crafts alkylation. Regarded as environmentally benign, its acidity and pore size decisively affect the catalytic activation and selectivity (Kim, Cho & Ryoo, 2014). Zeolites often possess shape-selectivity, so that only one isomer is formed. Xue *et al*. (2014) discuss the alkylation of ethylbenzene with diethyl carbonate over a modified HZSM-5 catalyst giving *para* selectivity (Figure 3). HZSM-5 zeolite is also commonly used in the synthesis of *p*-xylene through the alkylation of toluene. In a study by Zhang *et al.* (2014) it was found that the *p*-selectivity of their modified HZSM-5 catalyst was 91.2 %. By

modifying the zeolite with surface coatings of SiO_2, P_2O_5 and MgO, the *p*-selectivity could also be enhanced to 98 % (Tan *et al*., 2014).

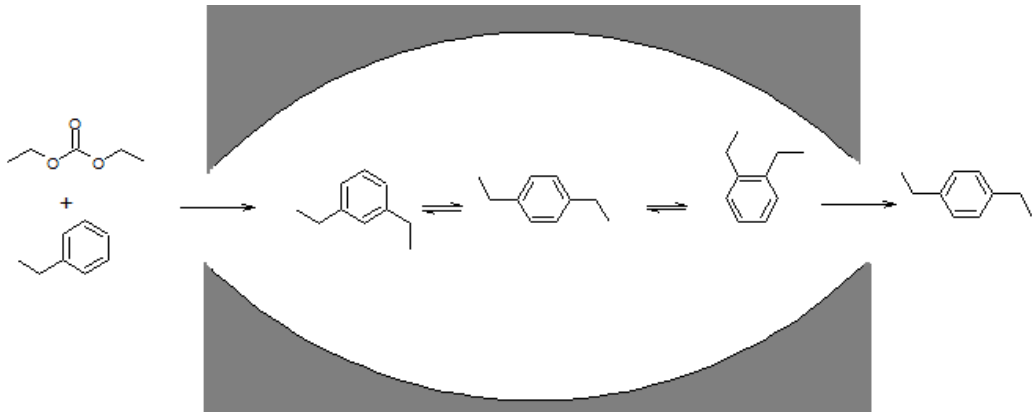

Figure 3: A graphical representation of the *para*-selectivity of HZSM-5 zeolite with the alkylation of ethylbenzene (Xue *et al.*, 2014)

However, due to the time and monetary constraints surrounding the project, the synthesis of a modified zeolite would not be a feasible route. Furthermore, by simply using a Lewis acid catalyst, the stereochemistry of the reaction could be better investigated and could prove to be more challenging.

With regards to the xylene used in the synthesis, Odochian *et al.* (2010) investigated the rates of alkylation of the three xylenes using *t*-butyl chloride. It was concluded that due to the para-directing nature of the methyl groups, *p*-xylene showed little to no evidence of a reaction occurring. On the other hand, *m*-xylene is stated to involve a site that is deactivated by the pre-existing substituents and hence the reaction rate is lower while *o*-xylene was concluded to have the highest reaction rate due to the pre-existing substituents being activating towards the substitution sites (Odochian *et al.*, 2010). However, as some literature accounts have stated previously that *o*-xylene will commonly isomerise when in the presence of the Lewis-Acid catalyst (Jin *et al*., 2013), *m*-xylene could provide simpler product predictions and also lead to a higher yield of mono-alkylated products. The work by Jin *et al.* (2013) suggests that a higher reaction temperature may be required to alkylate *m*-xylene.

Odochian *et al.* also demonstrated that whilst the alkylation of *m*-xylene was slower, the activation energy of *m*-xylene was in fact lower than that for *o*-xylene. This demonstrates how important the steric factor is concerning the reaction, and may allow greater insight into the predicted synthesised isomer.

Introducing a carbonyl group into the molecule could then also lead to subsequent reactions being performed, ultimately to reduce the carbonyl. One method to reduce the carbonyl group is hydrogenation using a palladium on carbon catalyst (Pd/C). This catalyst is the most frequently available heterogeneous hydrogenation catalyst in industry and academia and easily catalyses the hydrogenolysis of aromatic carbonyls to the methylene product (Hattori, Sajiki & Hirota, 2001). Palladium is most frequently used as its activity for ring saturation is low and high for the reduction of ketones (Rylander, 1979). In addition, the yield is usually high and the conditions employed are mild. It is often considered better than other chemical reductions such

as Clemmensen or Wolff-Kishner (Rylander, 1979). An example reaction scheme for the reduction is shown in Figure 4, displaying also the alcohol intermediate.

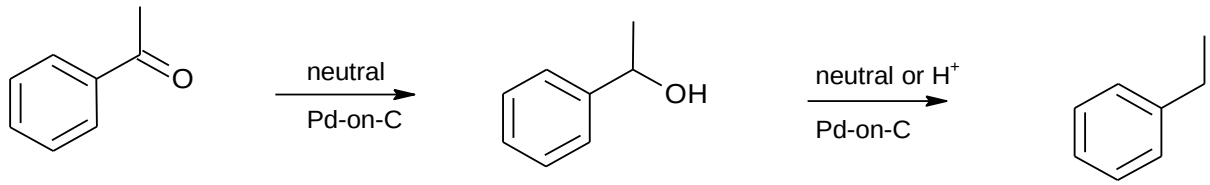

Figure 4: The reaction scheme for the hydrogenolysis of an aromatic ketone (acetophenone used as an example) using a Pd/C catalyst (Rylander, 1979)

The carbonyl could also be reduced in a multi-stage reaction. The Grignard reaction has the potential to synthesise hundreds of alcohols due to its incredibly broad scope. The Grignard reaction uses the Grignard reagent to reduce ketones to tertiary alcohols (March, 1992).

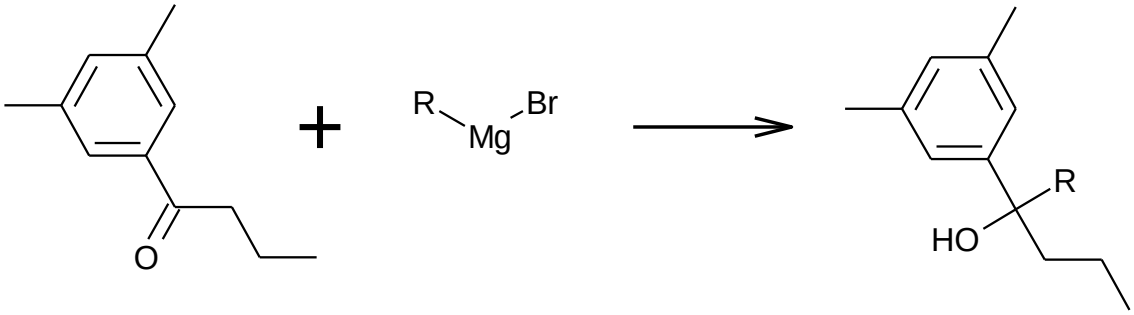

Figure 5: The reaction scheme for the reduction of the carbonyl to an alcohol using a Grignard reagent

The alcohol produced could then be further reduced in two consecutive steps. Dehydration of the alcohol could be performed using $POCl_3$ in mildly basic conditions with pyridine as a solvent, as demonstrated in Figure 6 (Patrick, 2000).

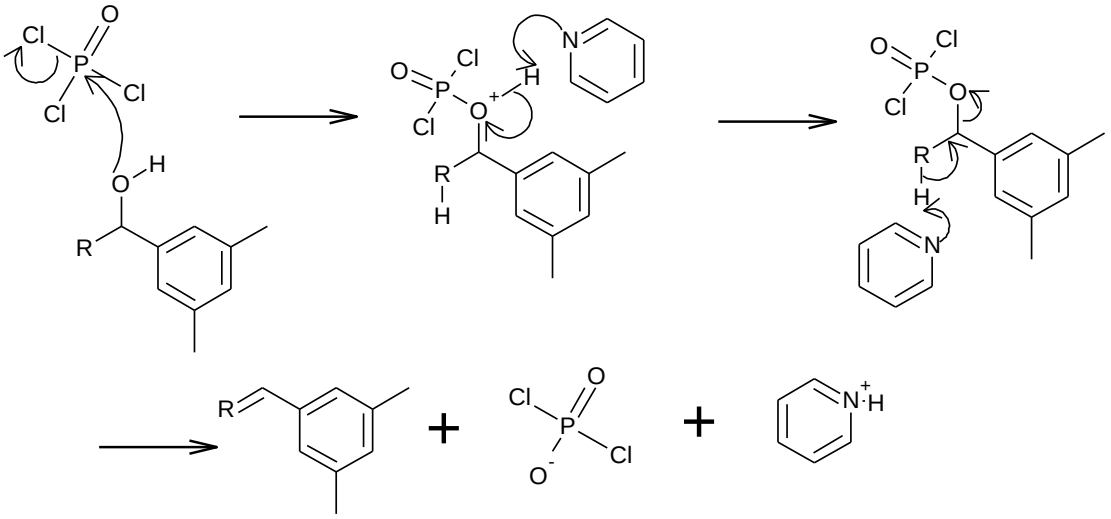

Figure 6: Dehydration using $POCl_3$

The alkene could then be hydrogenated to the final alkyl aromatic product. Alkenes are reduced easily. In fact the rate of hydrogenation using palladium, platinum, rhodium or nickel is so high that the rate is determined mostly by mass transport unless other precautions are taken (Rylander, 1979). The final product could therefore be hydrogenated again using a Pd/C catalyst.

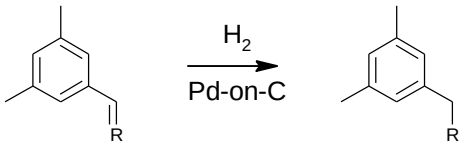

Figure 7: The reaction scheme for the reduction of the olefin using a Pd/C catalyst

The aim of this project was the synthesis and characterisation of an alkyl-xylene, allowing challenging synthetic and analytical techniques to be used. The comparison of Friedel-Crafts alkylation and acylation will be discussed, with an attempt to reduce the carbonyl of the acyl-aromatic to yield a comparable alkyl-aromatic. Characterisation of the products will include appropriate spectral analysis such as infra-red and NMR spectroscopy, gas chromatography-flame ionisation detector and gas chromatography-mass spectrometry.

Experimental

Friedel-Crafts alkylation

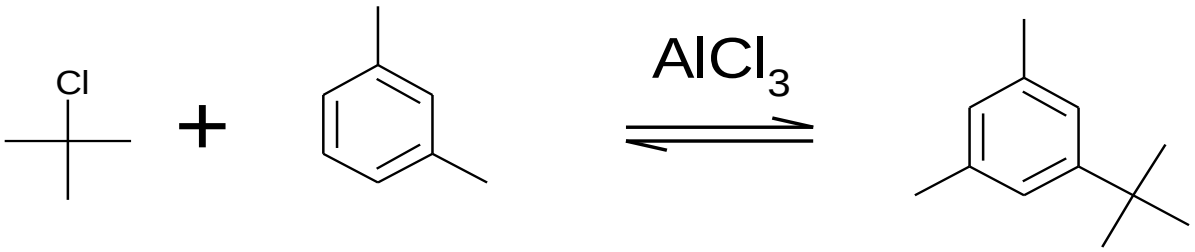

Figure 8: The reaction scheme for the Friedel-Crafts alkylation of *m*-xylene using *t*-butyl chloride

Anhydrous aluminium chloride (1.05 g) and *m*-xylene (60 mL) were measured into a 250 mL 3-necked round bottom flask. The flask was equipped with a thermometer, a pressure equalising dropping funnel and a condenser attached to a calcium guard tube. *t*-Butyl chloride (10 mL) was added to the dropping funnel, and the round bottom flask was heated (60 °C) using a heating mantle.

The *t*-butyl chloride was added drop-wise to the *m*-xylene solution over an hour period with the temperature of the solution maintained between 55 - 65 °C. The solution turned dark brown to black in colour. After this hour period, the heater was switched off and the solution was left to stir (2 h).

Crushed ice (*ca.* 100 g) was added gradually to the stirring solution and once the ice had melted, the solution was poured into a 250 mL separating funnel. Concentrated HCl (37 %; *ca.* 20 mL) was then added to the separating funnel and two distinct layers formed.

The top organic layer was extracted and washed with three aliquots of milli-Q water. This layer was then transferred to a 150 mL conical flask and dried over anhydrous calcium chloride.

The product was then purified using vacuum distillation. The product was collected at 106 °C at 30 mmHg and appeared as a clear, oily liquid.

Friedel-Crafts acylation

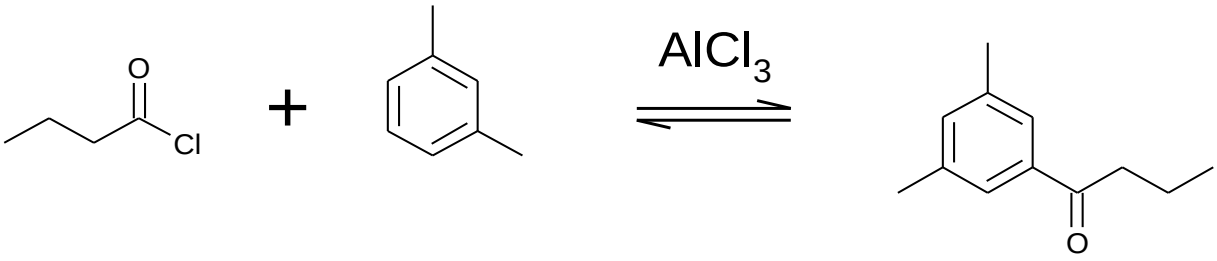

Figure 9: The reaction scheme for the Friedel-Crafts acylation of *m*-xylene using butyryl chloride

All glassware was dried in an oven at 170 °C for 1 hour prior to use. A 250 mL round bottom flask was equipped with a condenser, attached to a calcium guard tube and two pressure equalising dropping funnels. To the round bottom flask, dichloromethane (20 mL) and anhydrous aluminium chloride (7.95 g) was added along with a PTFE stirrer. This was then placed in an ice bath and stirring was initiated. To one dropping funnel, butyryl chloride (4 mL) and dichloromethane (10 mL) were added. This was then added to the round bottom flask slowly (15 min) to give a cloudy, yellow solution. To the other dropping funnel, *m*-xylene (4.5 mL) and dichloromethane (10 mL) were added. This was then slowly added to the round bottom flask (15 min)

The ice bath was removed once all of the *m*-xylene had been added and the solution was left stirring (15 min), giving a translucent brown solution. The contents of the round bottom flask were transferred to a 600 mL beaker containing concentrated HCl (37 %; 40 mL) and crushed ice (*ca.* 50 g). This was then stirred (30 min) to yield a cloudy white solution. The organic layer of the solution was then extracted using a liquid-liquid extraction in a 250 mL separating funnel. The upper aqueous layer was washed with dichloromethane (2 x 15 mL); combining the DCM extracts and discarding the aqueous layer. The DCM extracts were then washed with NaOH (10 %; 2 x 15 mL) and milli-Q water (2 x 15 mL). The DCM extracts were then poured into a conical flask and dried over anhydrous calcium chloride. The product was then filtered under gravity through grade 1, 11 µm fluted filter paper into a pre-weighed round bottom flask.

Rotary evaporation was performed using a water bath (45 °C) until masses measured between evaporations became concordant. The product was a pale yellow, oily liquid.

Grignard reaction

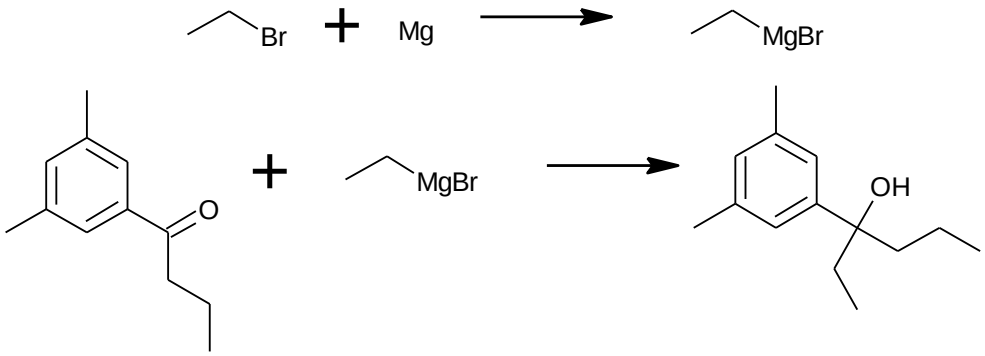

Figure 10: The reaction scheme for the formation of the Grignard reagent using ethyl bromide and then its reaction with the acyl xylene

All glassware was dried in an oven at 170 °C for 1 hour prior to use. A 100 mL three-necked round bottom flask was attached to a condenser and pressure equalising dropping funnel and a calcium guard tube was attached to the top of the condenser. To the round bottom flask, magnesium turnings (0.44 g) were added with dry ether (10 mL). To the dropping funnel, bromoethane or 1-bromopropane (1.08 g or 4.62 g, respectively) in dry ether (3 mL) were added. The apparatus was placed into a bowl of warm water and a small amount of the bromopropane solution was run into the round bottom flask to initiate the reaction. The remainder of the dropping funnel was added drop-wise at such a rate that gentle reflux was maintained.

The reaction was then transferred to an ice bowl to cool and a solution of acyl-*m*-xylene (1.5 g for the ethyl bromide, 5.01 g for the propyl bromide) in dry ether (3 mL) was added. After the addition, the reaction was stirred continuously (10 min). The reaction mixture was then gently refluxed (10 min) using a bowl of warm water. The reaction mixture was then cooled and poured onto crushed ice (*ca.* 50 g) in a 250 mL beaker whilst being stirred gently with a glass rod. Saturated ammonium chloride (5 mL) was then added.

The inside of the round bottom flask was rinsed with dry ether, which was added to the contents of the beaker. This was then transferred to a 250 mL separating funnel. The upper ether layer was extracted and the lower aqueous layer was washed twice with ether (20 mL). The ether extracts were combined and dried over anhydrous potassium carbonate (20 min). The ether solution was filtered under gravity through grade 1, 11 µm fluted filter paper into a pre-weighed round bottom flask. The ether was removed by rotary evaporation until masses between runs were concordant.

IR spectroscopy analysis

IR analysis was performed using a Bruker Alpha FT-IR Spectrometer with Platinum ATR module. 16 scans were performed at 4 cm^{-1} resolution using a DTGS detector.

GC-FID analysis

All samples were diluted to within a concentration range of 200 - 400 mg L^{-1} using dichloromethane as a solvent. Samples were analysed using an Agilent 7890A GC equipped with a 7683 Series Autosampler and 7683B Series Autoinjecter (temperature 250 °C). The stationary phase was an HP5 low polarity column (30 m x 0.320 mm internal diameter with 0.25 µm film thickness). The carrier gas was

nitrogen with a flow rate of 1.0 mL min^{-1}. All samples were analysed using the 'General method' with a temperature range of 40 - 300 °C at 10 °C min^{-1} and then held at 300 °C for 10 minutes.

The GC was equipped with a flame ionisation detection held at 300 °C with a hydrogen flow rate of 40 mL min^{-1} and an airflow rate of 400 mL min^{-1}. The nitrogen (make-up) flow rate was 15 mL min^{-1}.

The software used to analyse the chromatograms was ChemStation™ (Revision B.03.01, May 2007).

GC-MS analysis
All samples were diluted to within a concentration range of 20 - 40 mg L^{-1} using dichloromethane as a solvent. Samples were analysed using an Agilent 7890A GC equipped with a 7683B Series autosampler and a 5975A quadrupole mass selective detector. The stationery phase was an HP-5MS fused silica capillary column (30 m x 0.25 mm internal diameter with 0.25 µm film thickness). The carrier gas was helium with a constant flow of 1.0 mL min^{-1}. A splitless injector was used at 300 °C with sample volumes of 1.0 µL. The oven temperature range was 40 - 300 °C at 10 °C min^{-1} and was then held at 300 °C for 10 min.

The quadrupole mass spectrometer had an ion source temperature of 280 °C and used ionisation energy of 70 eV. The instrument was operated in full scan mode with a mass range of 50 - 550 Daltons being monitored. The software used to monitor and record all data and chromatograms was ChemStation™ (Revision E.01.00.237).

NMR spectroscopy analysis
Samples were analysed using a JNM-LA400 FT spectrometer (JEOL USA, Inc) operating at 400 MHz. The software used was Delta NMR Software V.4.3.5. The experiments performed were proton (^{1}H), carbon-13 (^{13}C) and distortionless enhancement by polarization transfer (DEPT).

Results

Friedel-Crafts alkylation

Table 1: The theoretical and actual yield for the alkylation of *m*-xylene using *t*-butyl chloride

Theoretical yield (g)	Actual yield (g)	Per cent yield (%)
14.71	9.55	65

The following spectra and analysis were obtained from the product of the Friedel-Crafts alkylation of *m*-xylene with *t*-butyl chloride.

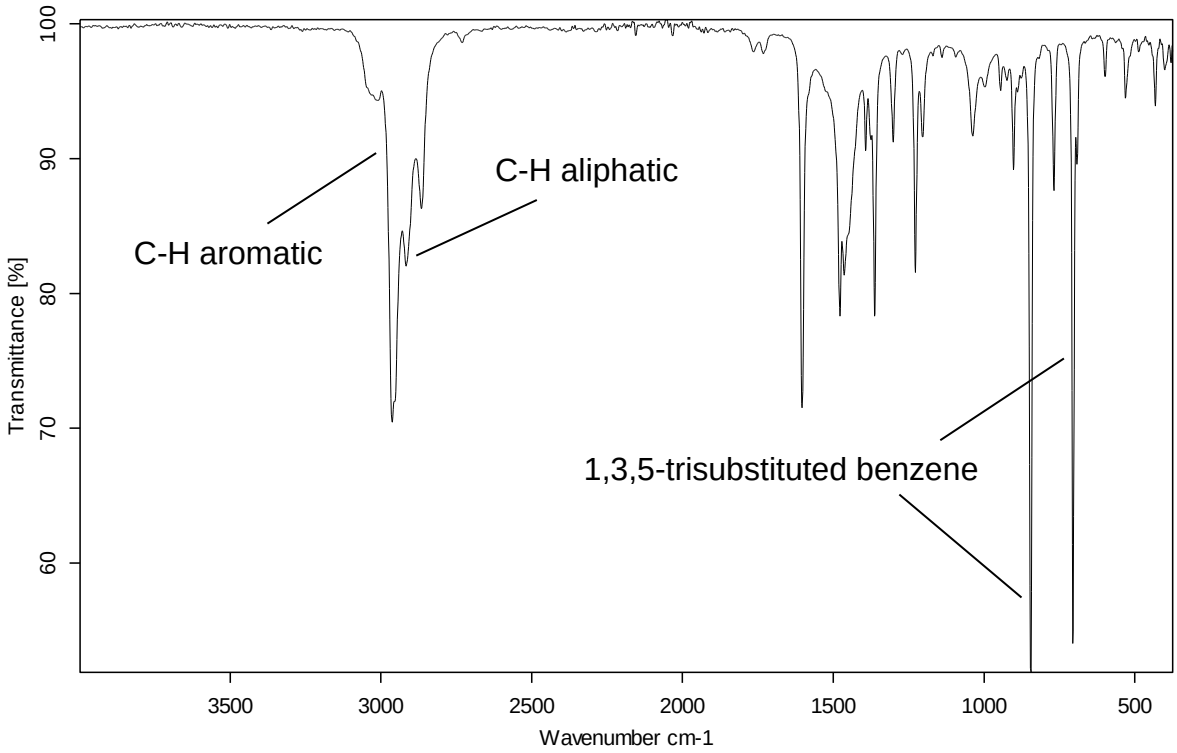

Figure 11: The infrared spectrum of the Friedel-Crafts alkylation reaction with *m*-xylene

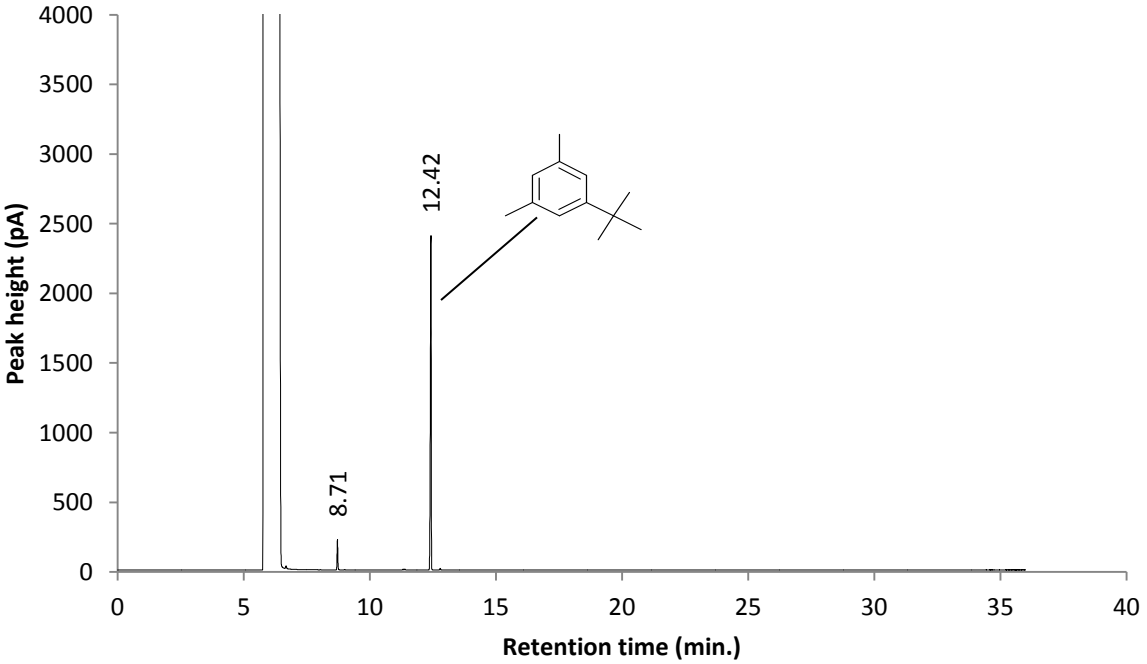

Figure 12: Gas chromatogram of the product of the Friedel-Crafts alkylation reaction with *m*-xylene

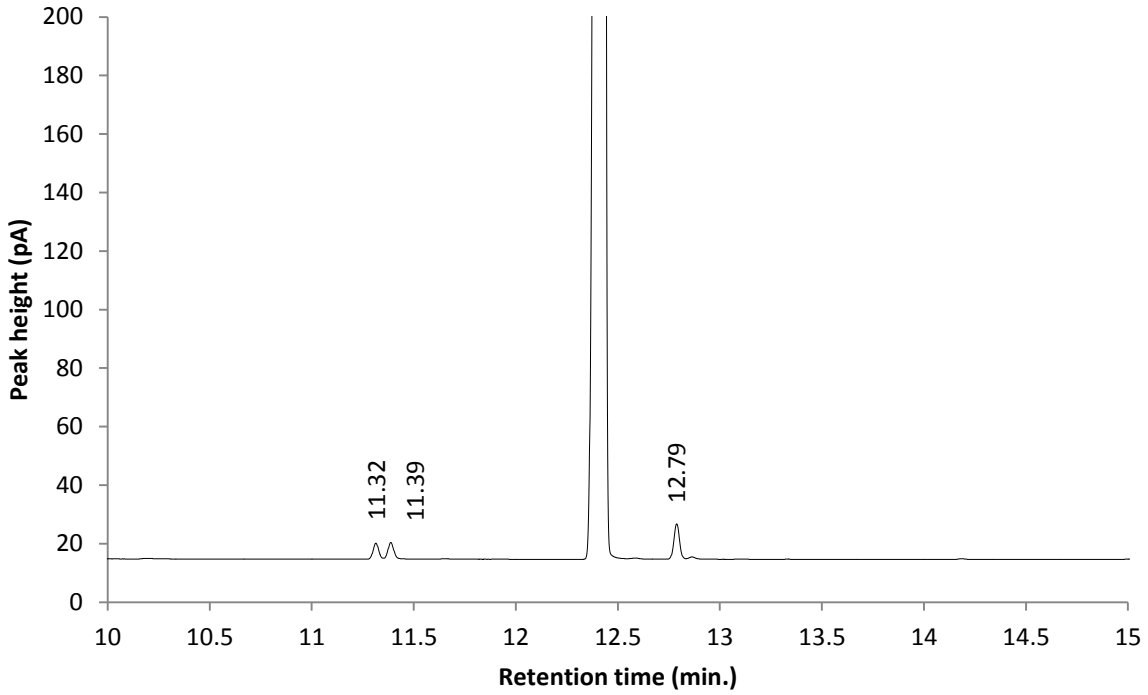

Figure 13: Gas chromatogram in Figure 12 at a higher magnification of the peak at 12.42 minutes to allow the observation of the smaller peaks either side

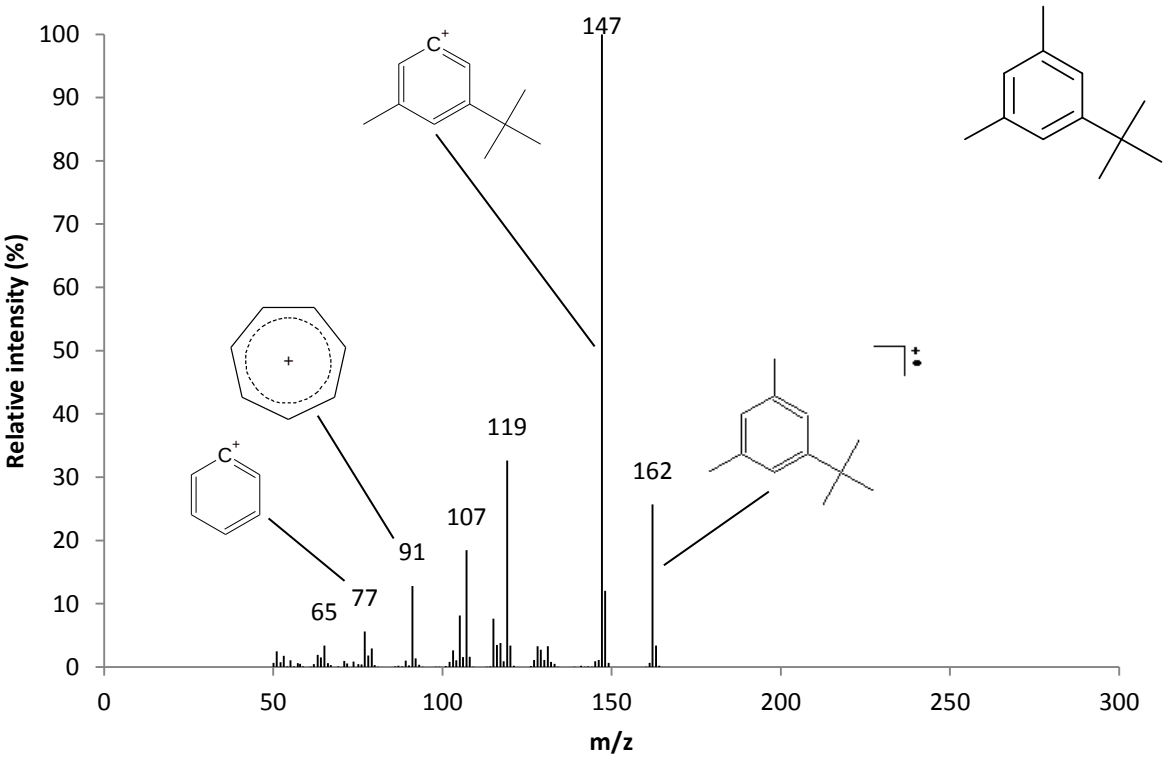

Figure 14: Mass spectrum for the predominant product peak at 12.42 minutes

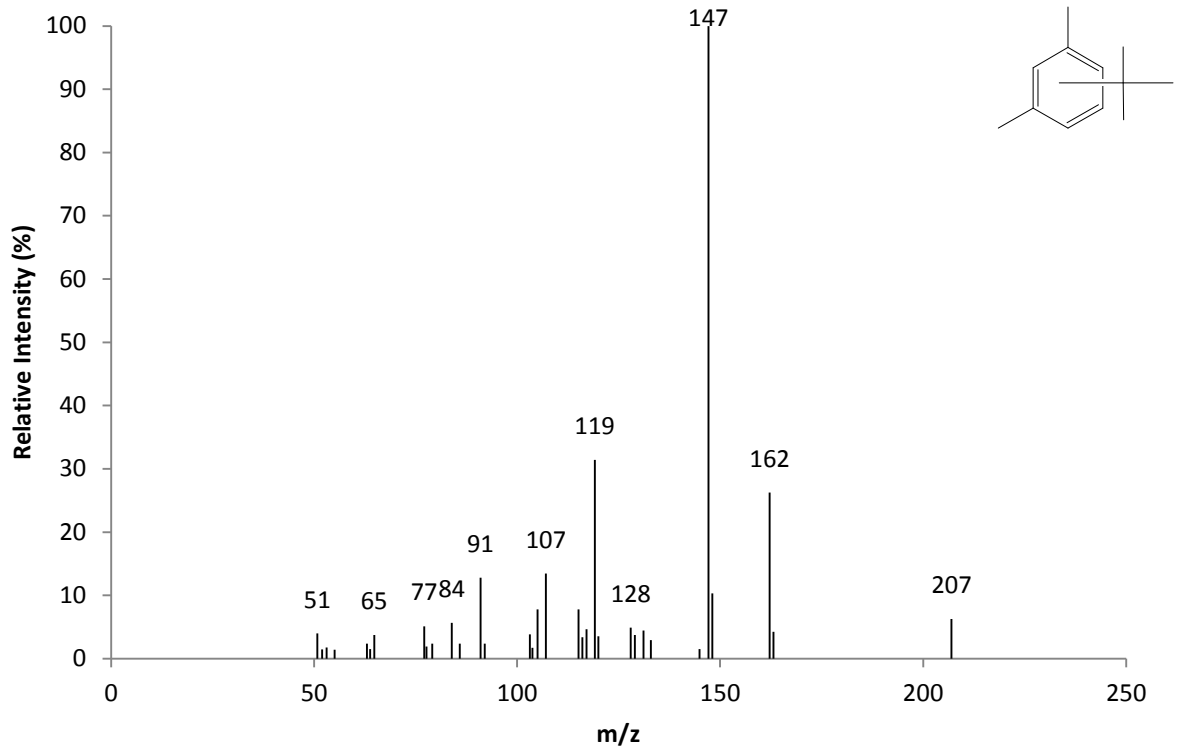

Figure 15: Mass spectrum for the smaller peak at 12.79 minutes showing a similar fragmentation pattern to the predominant product peak

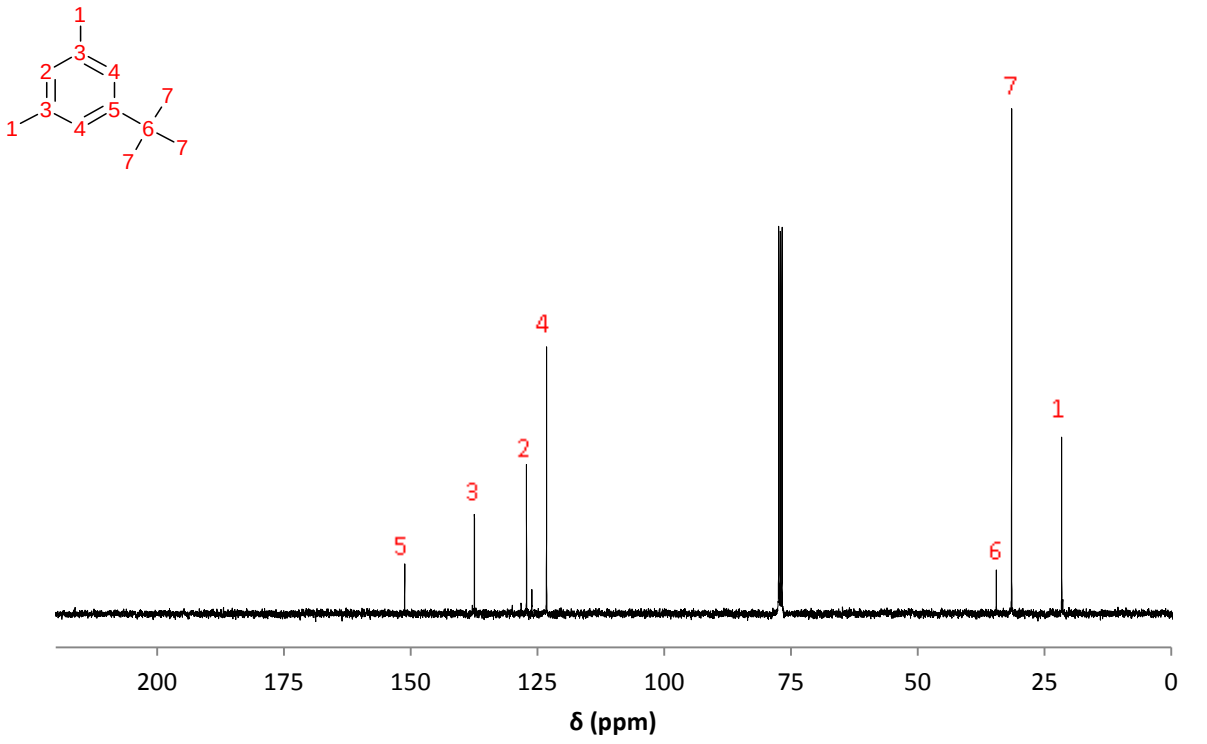

Figure 16: ^{13}C NMR spectrum of the product of the Friedel-Crafts alkylation reaction with *m*-xylene

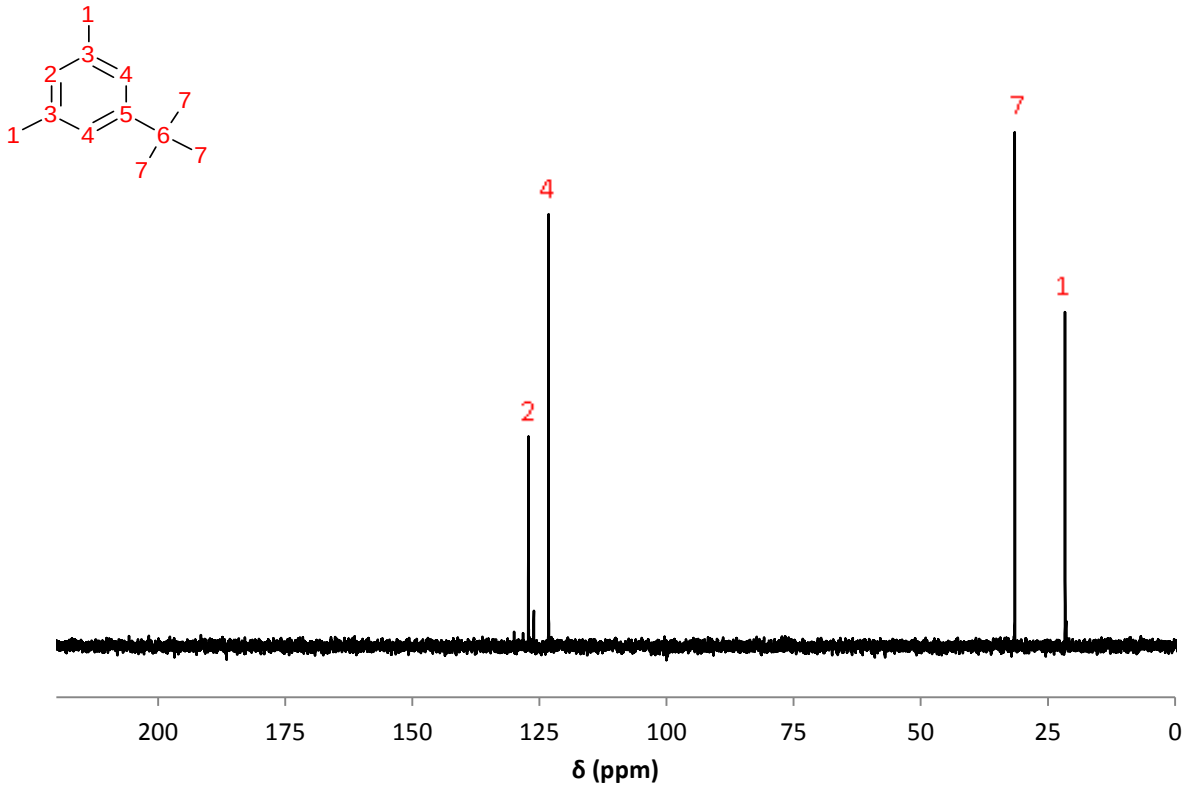

Figure 17: DEPT NMR spectrum of the product of the Friedel-Crafts alkylation reaction with *m*-xylene

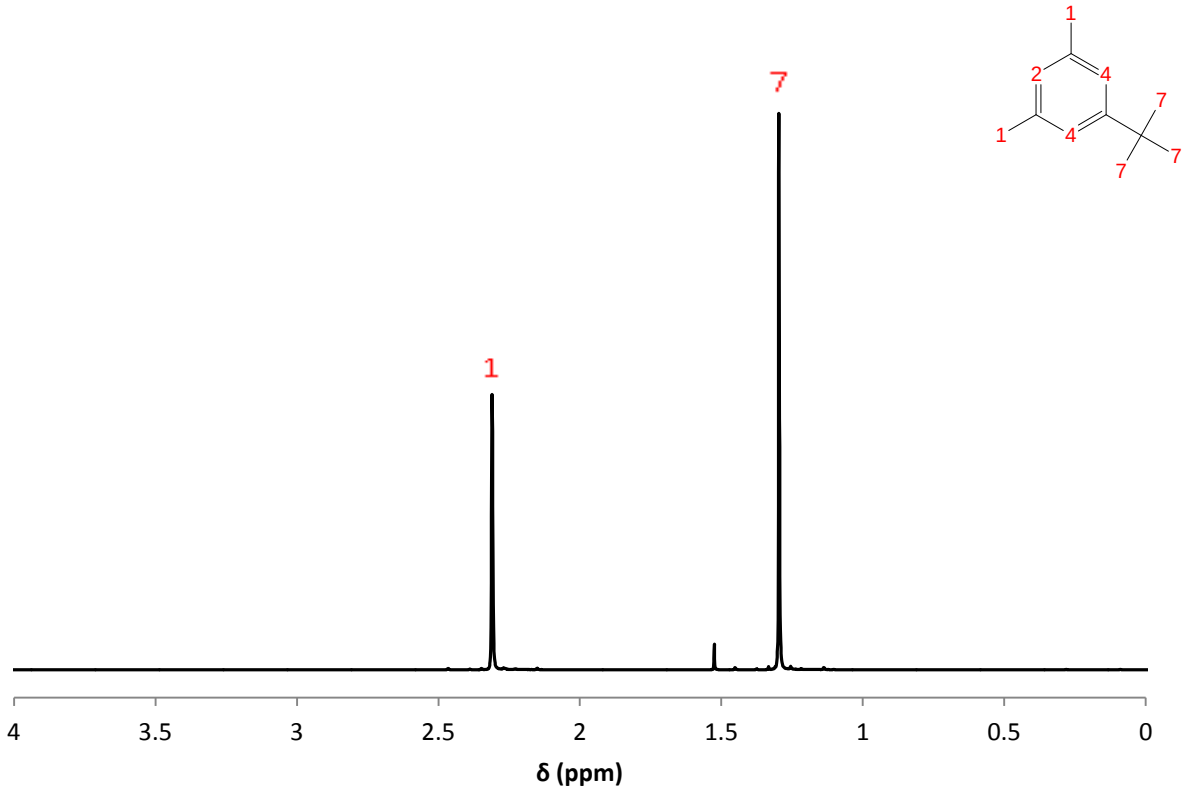

Figure 18: The ^{1}H proton NMR spectrum of the product of the Friedel-Crafts alkylation of *m*-xylene showing the aliphatic proton peaks

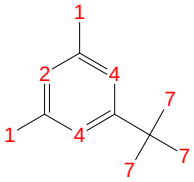

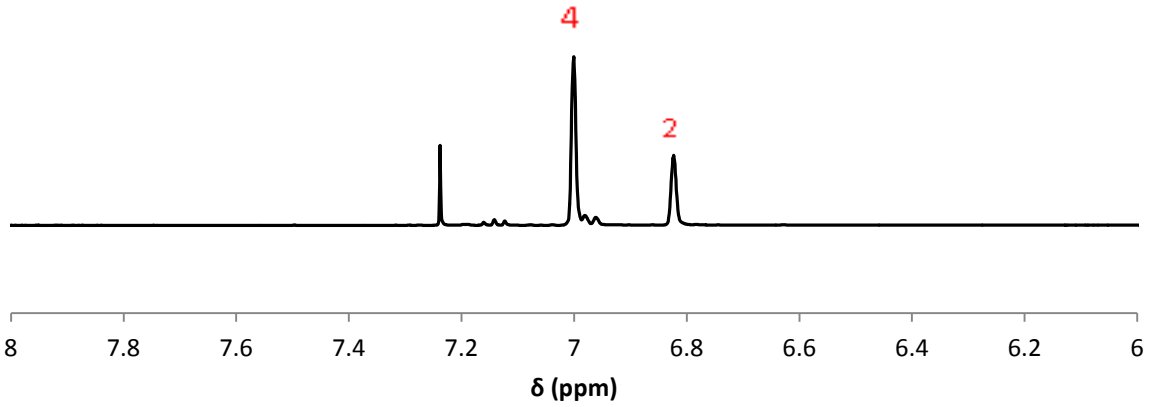

Figure 19: The ^{1}H proton NMR spectrum of the alkylation product showing the aromatic proton peaks

Friedel-Crafts acylation

Table 2: The theoretical and actual yield for the acylation of *m*-xylene using butyryl chloride

Theoretical yield (g)	Actual yield (g)	Per cent yield (%)
12.85	10.54	82.02

The following spectra and chromatograms were obtained from the product of the Friedel-Crafts acylation of *m*-xylene with butyryl chloride.

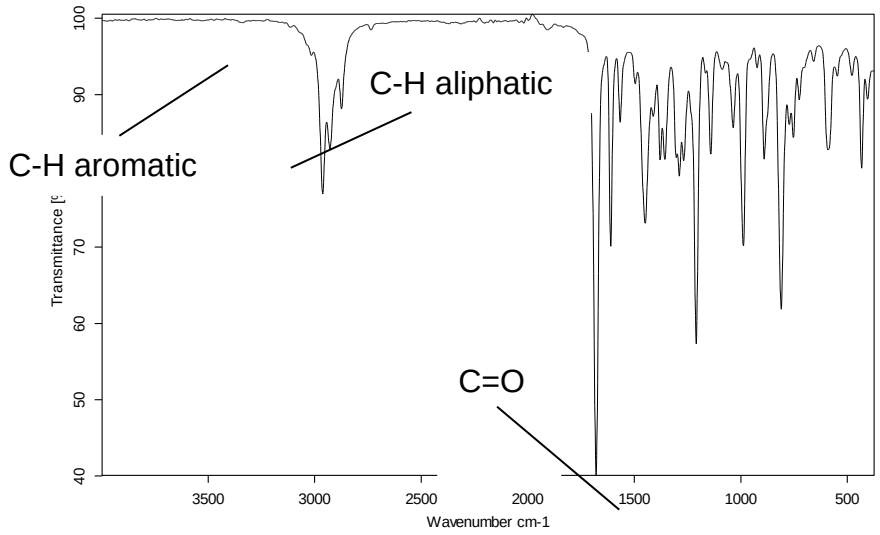

Figure 20: The infrared spectrum of the product of the Friedel-Crafts acylation of *m*-xylene

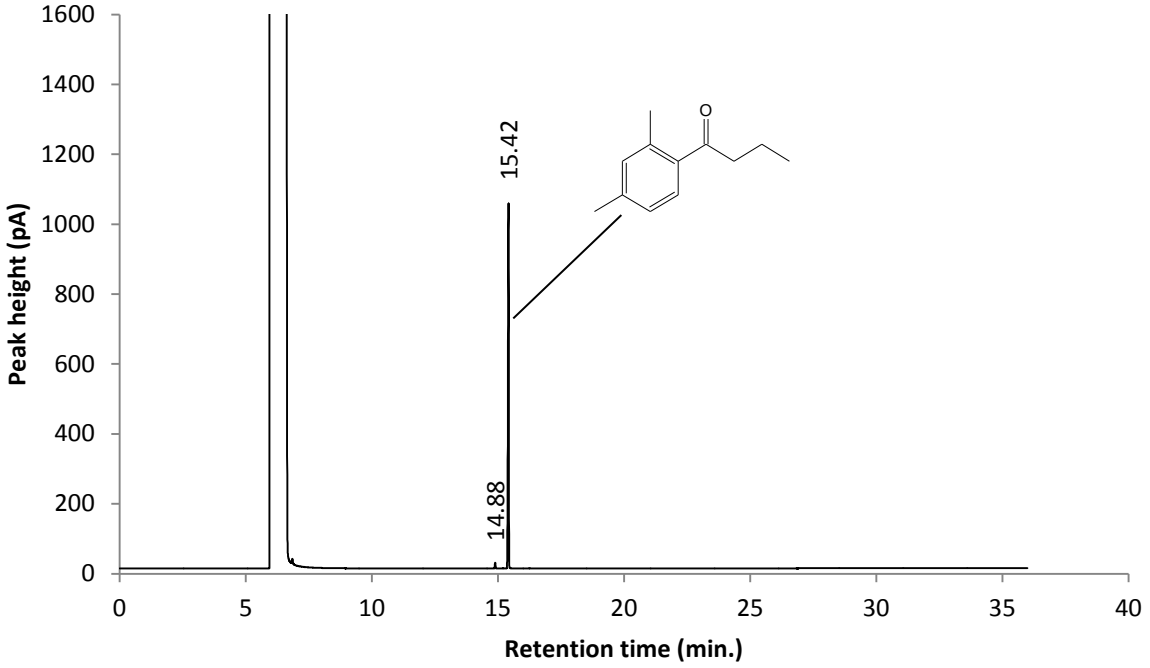

Figure 21: Gas chromatogram of the product of the Friedel-Crafts acylation of *m*-xylene

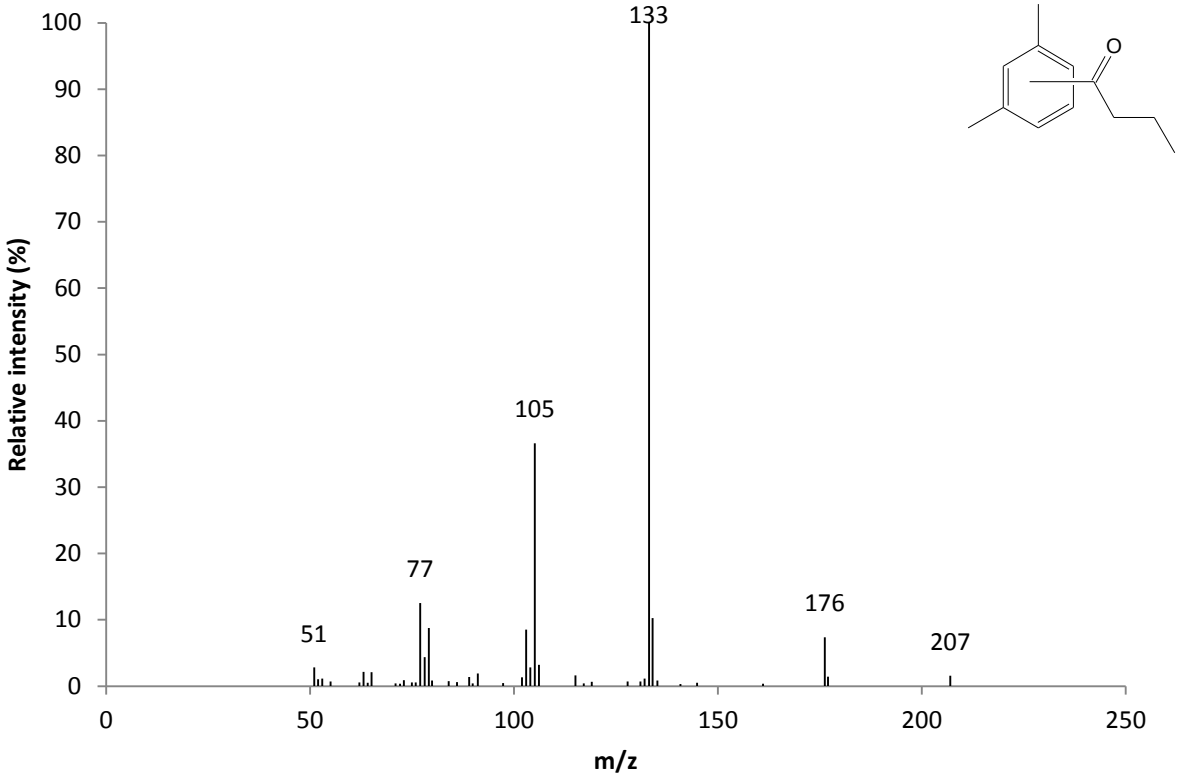

Figure 22: Mass spectrum for the minor peak at 14.88 minutes

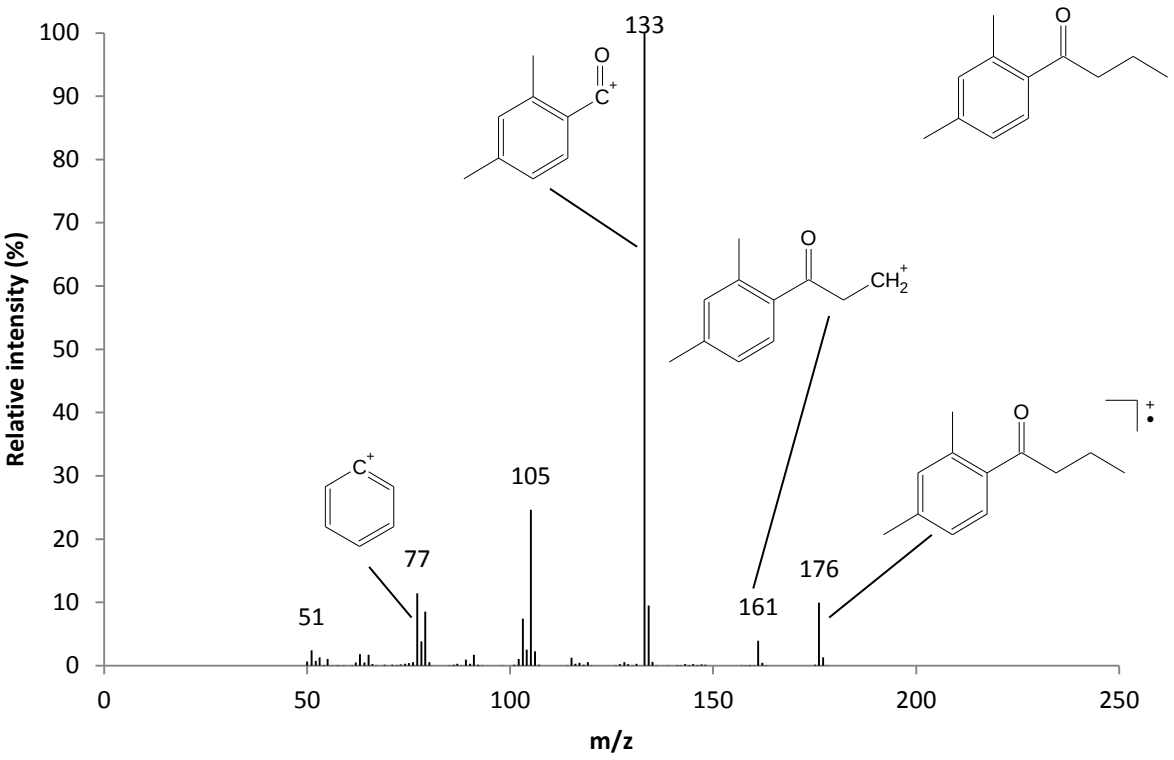

Figure 23: Mass spectrum for the major peak at 15.42 minutes

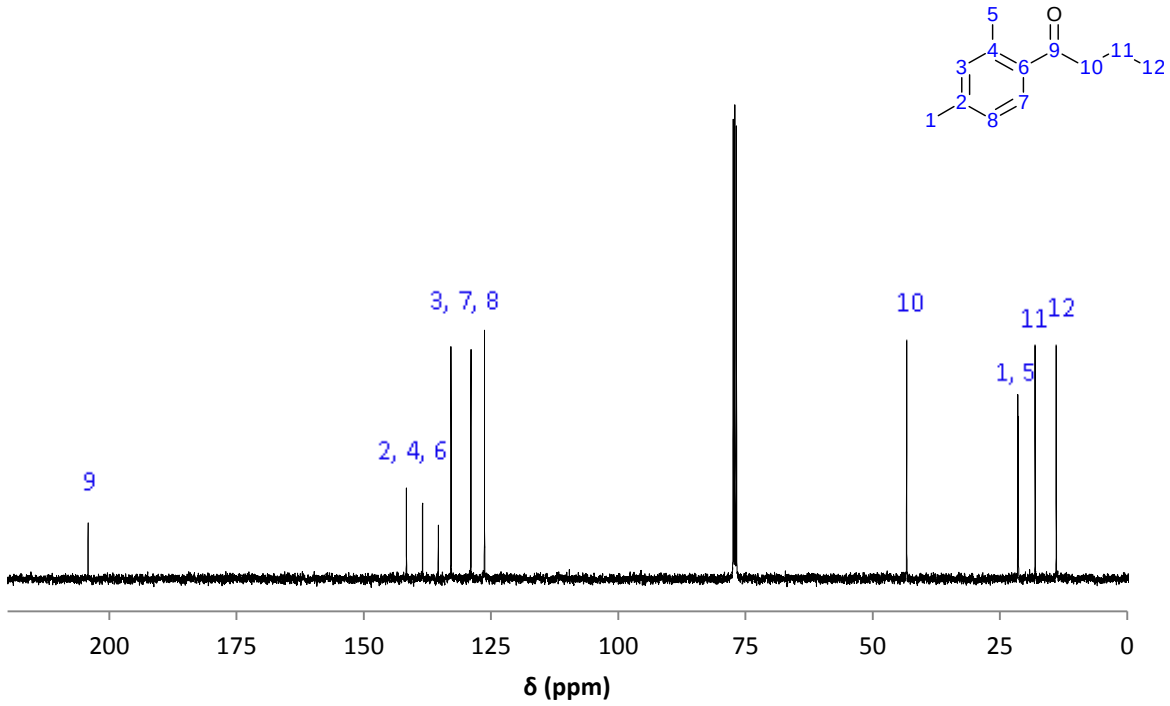

Figure 24: ^{13}C NMR spectrum of the product of the Friedel-Crafts acylation of *m*-xylene

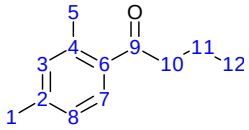

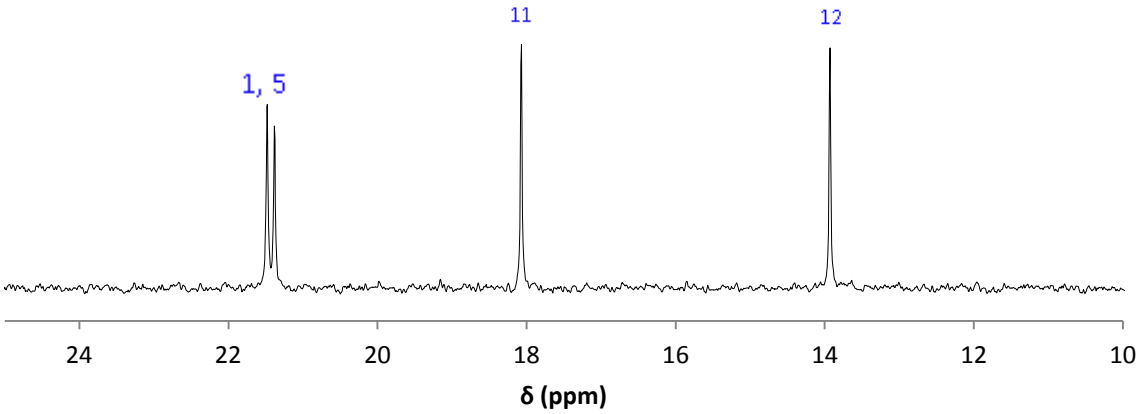

Figure 25: ^{13}C NMR spectrum of the Friedel-Crafts acylation product at a larger magnification to show the presence of two peaks between 21 and 22 ppm

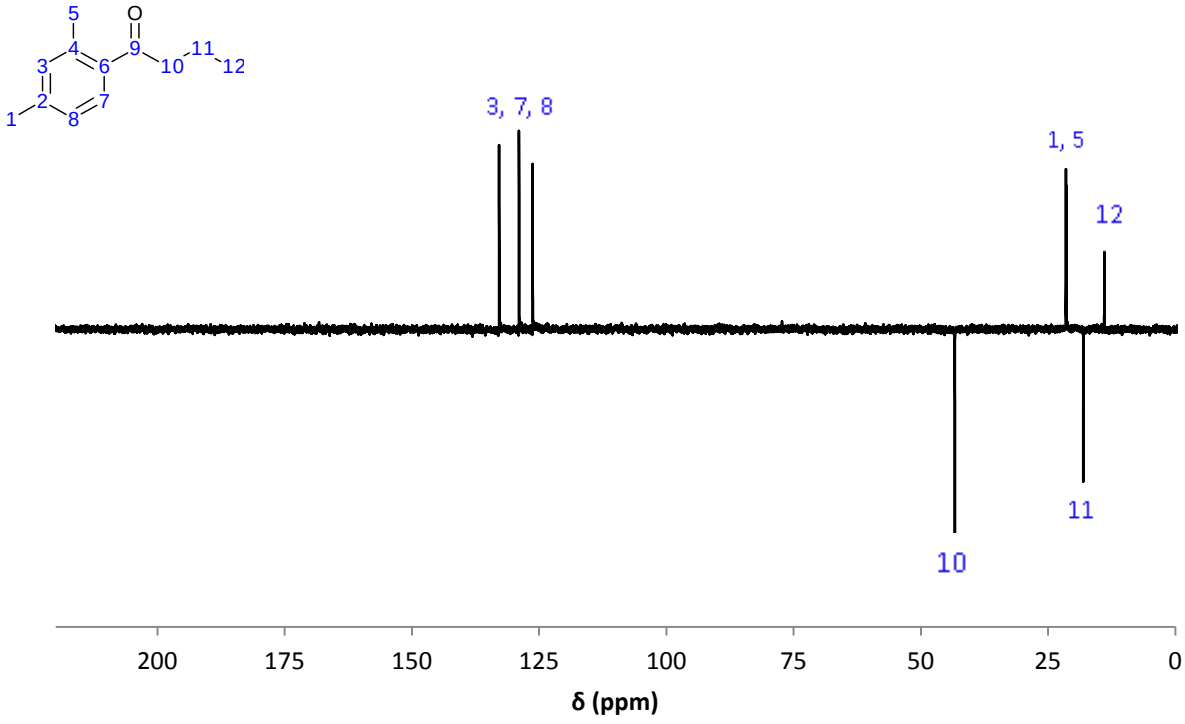

Figure 26: DEPT NMR spectrum of the product of the Friedel-Crafts acylation of *m*-xylene

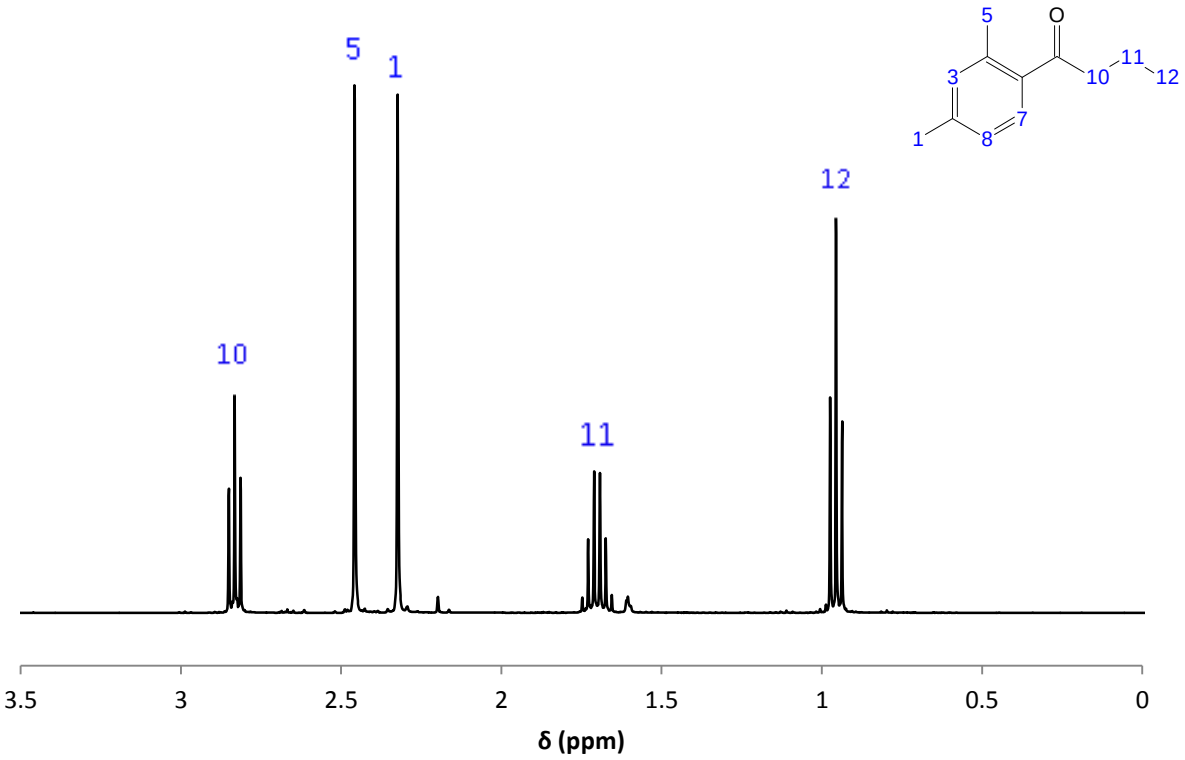

Figure 27: ^{1}H proton NMR spectrum of the product of the Friedel-Crafts acylation of *m*-xylene showing the aliphatic protons

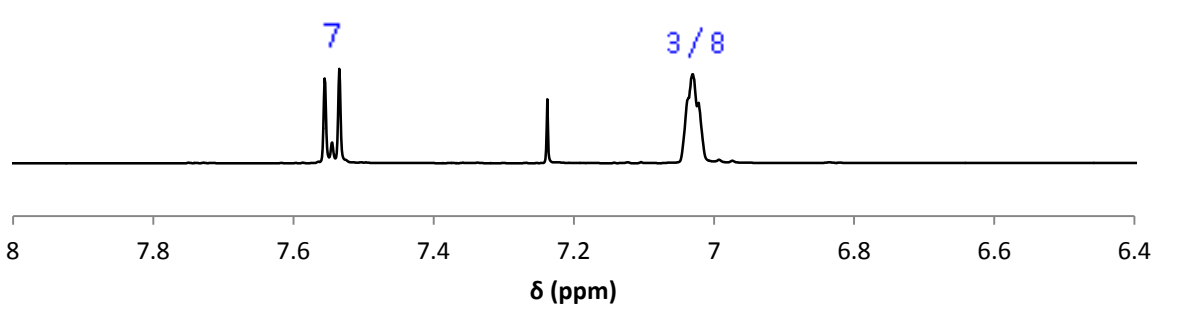

Figure 28: ^{1}H proton NMR spectrum showing the aromatic proton peaks of the acylation product

Grignard reaction of the acyl xylene with ethyl bromide

Table 3: The theoretical and actual yield for the Grignard reaction of the acyl-xylene with magnesium and ethyl bromide

Theoretical yield (g)	Actual yield (g)	Per cent yield (%)
2.43	0.03	1.2

The following spectra and chromatograms were obtained from the product of the Grignard reaction of the acyl xylene with ethyl bromide and magnesium.

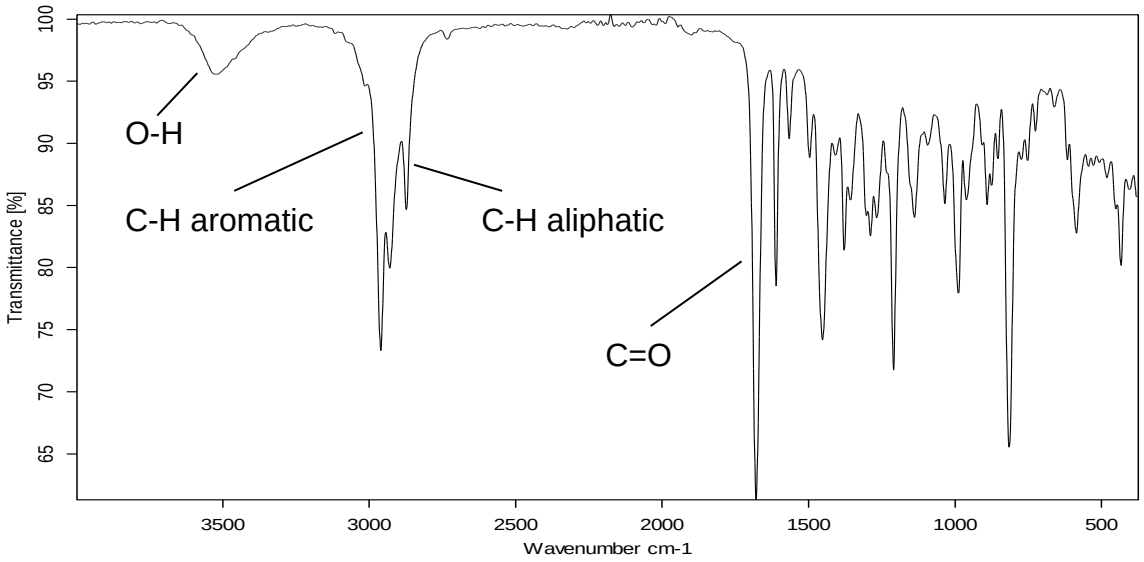

Figure 29: The infrared spectrum of the Grignard reaction of the acylation product with ethyl bromide

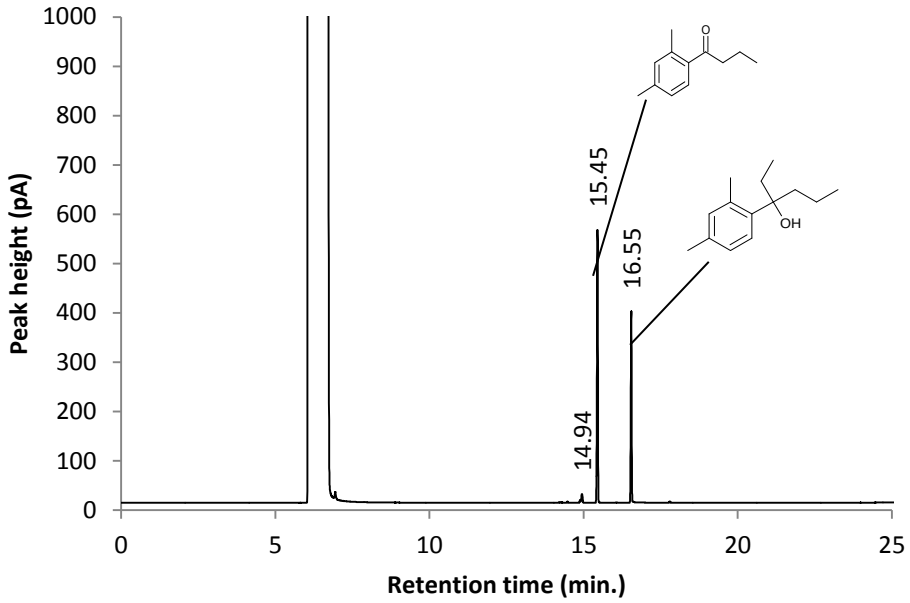

Figure 30: Gas chromatogram of the Grignard reaction of the acylation product with ethyl bromide

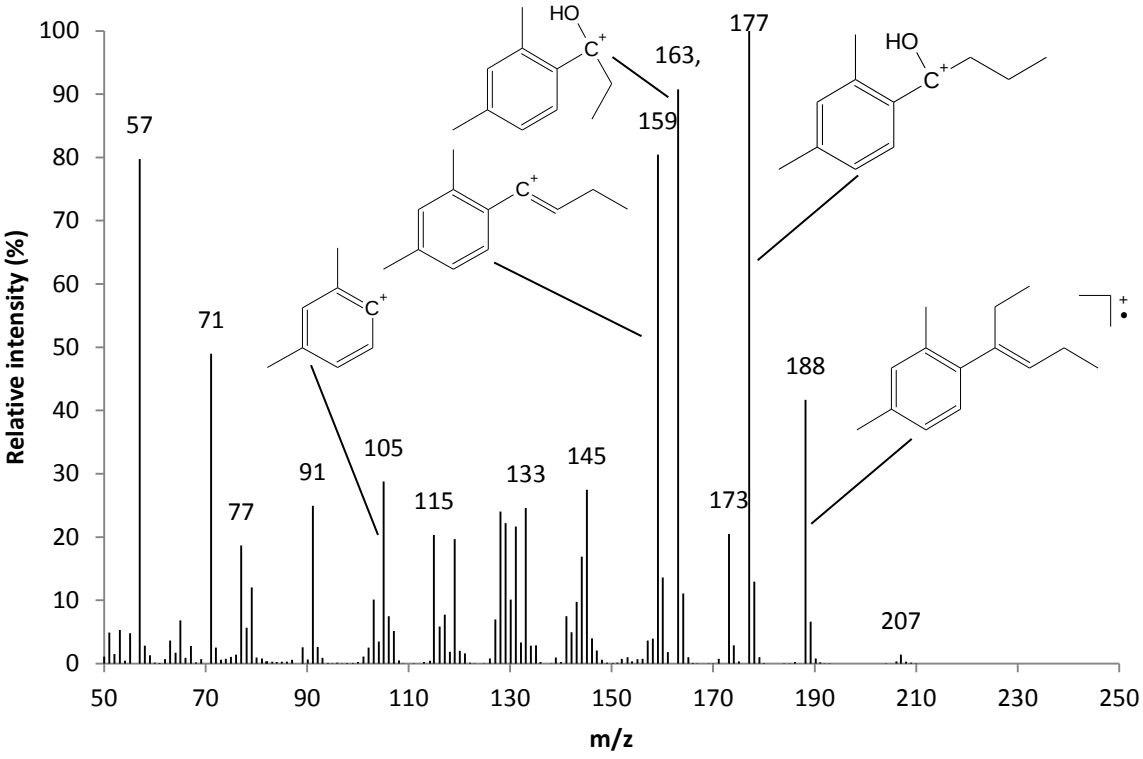

Figure 31: Mass spectrum of the alcohol peak at 16.55 minutes

Grignard reaction of the acyl xylene with propyl bromide

Table 4: The theoretical and actual yield for the Grignard reaction of the acyl-xylene with magnesium and propyl bromide

Theoretical yield (g)	Actual yield (g)	Per cent yield (%)
6.28	4.50	71.7

The following spectra and chromatograms were obtained from the Grignard reaction of the acyl xylene with propyl bromide.

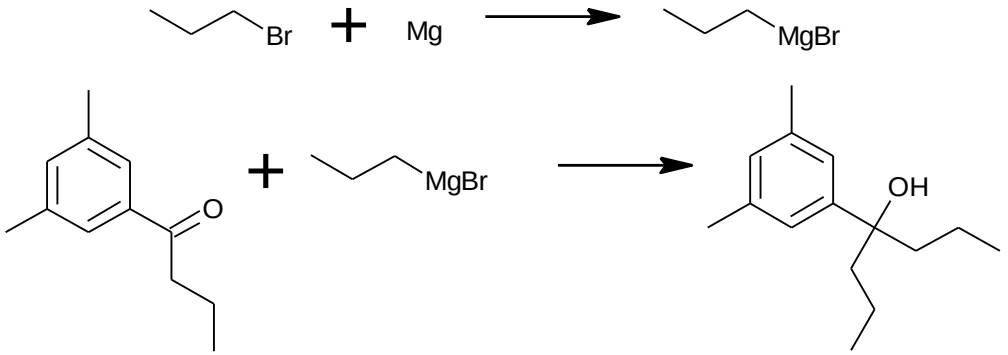

Figure 32: The reaction scheme for the formation of the Grignard reagent using propyl bromide and then its reaction with the acyl xylene

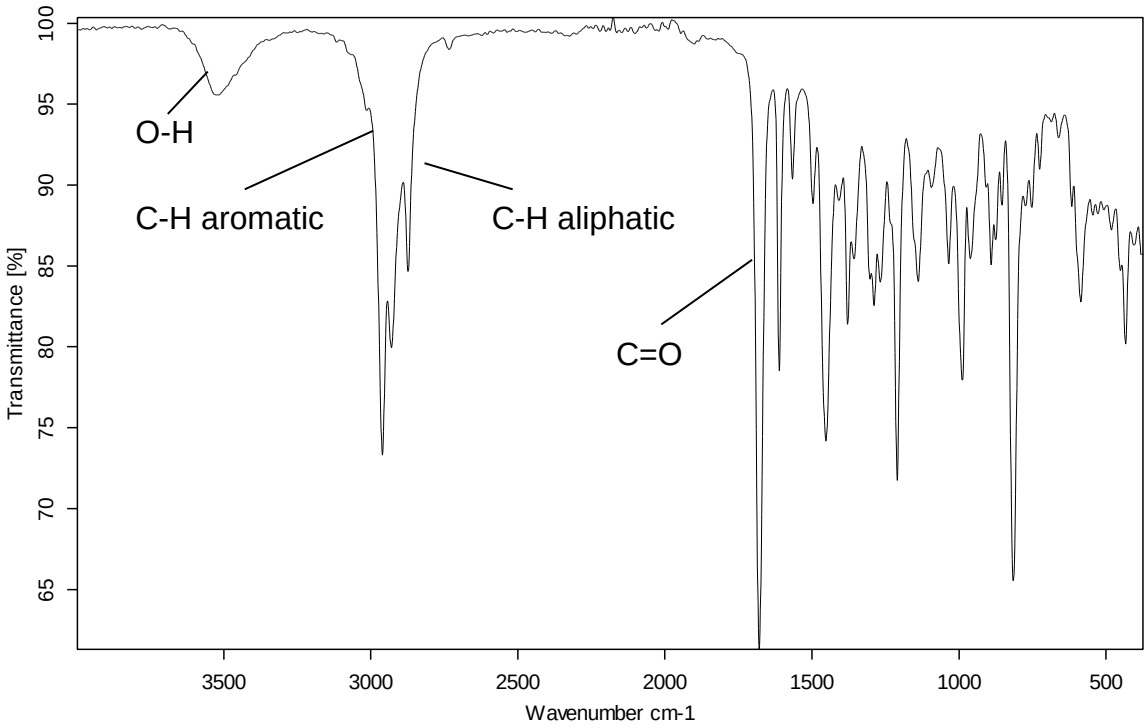

Figure 33: The infrared spectrum of the Grignard reaction of the acylation product with propyl bromide

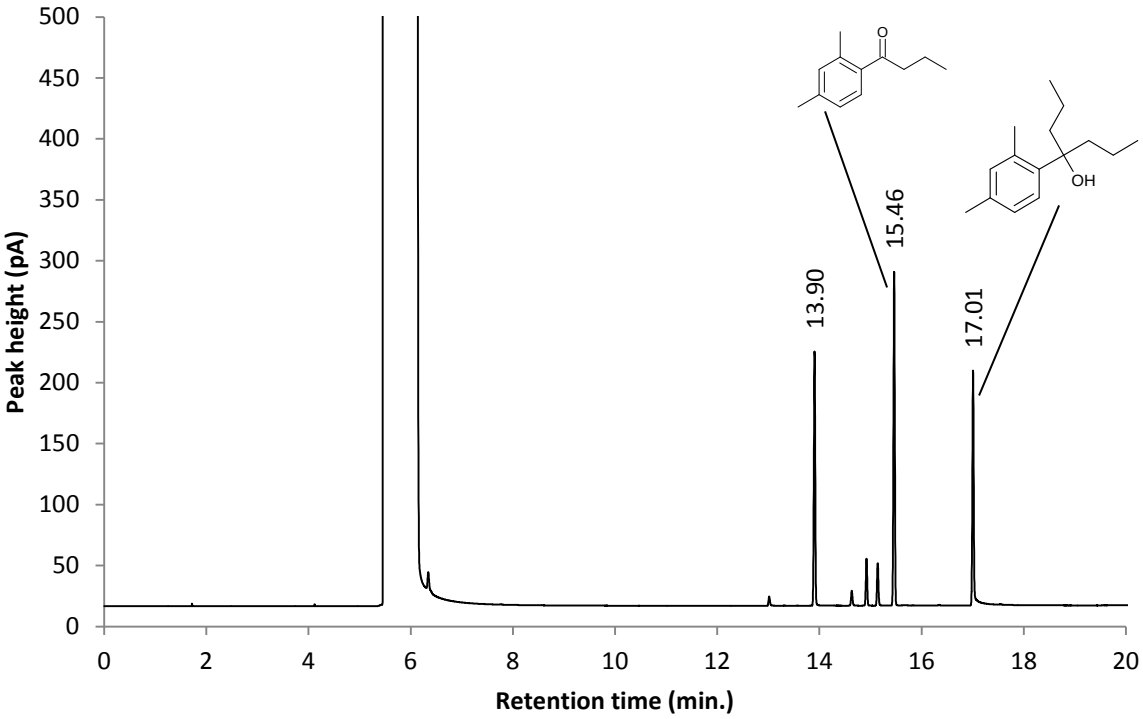

Figure 34: Gas chromatogram of the Grignard reaction of the acylation product with propyl bromide

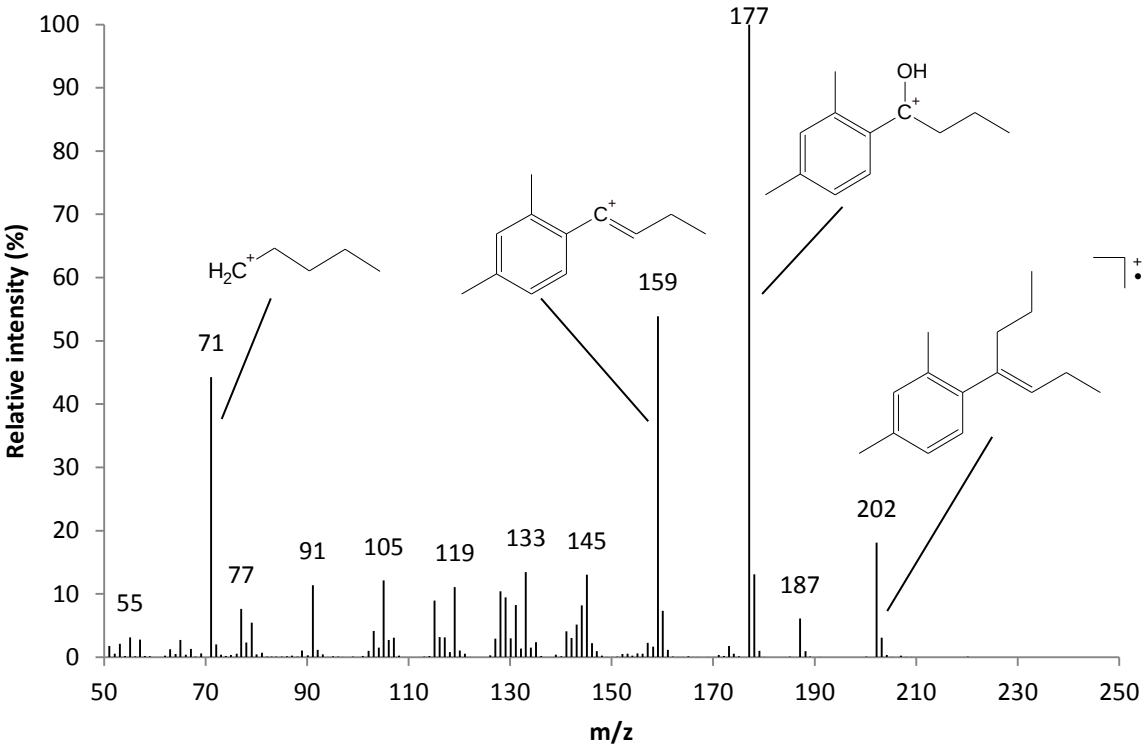

Figure 35: Mass spectrum produced from the alcohol formed from the Grignard reaction with propyl bromide (retention time 17.01 min.)

Discussion

Friedel-Crafts alkylation

The yield for the Friedel-Crafts alkylation was low at 64.91 %. This is most likely because the crude product was not distilled to completion and there was a lot of product remaining in the initial round bottomed flask. This was due to the worry of loss of product or the introduction of impurities. The chromatogram of the product initially showed a purity of 82.8 %. GC-FID allowed the assignment of the major impurity to *m*-xylene and due to the large difference in boiling points between this and the product, rotary evaporation allowed further purification. The subsequent GC-FID showed a higher purity of 92.7 %, allowing further analysis by NMR and IR spectroscopy.

Initial analysis using IR spectroscopy shows several peaks in the range of 3014 - 2866 cm^{-1} that are typical of both aliphatic and aromatic C-H stretches -- the *t*-butyl groups show characteristic stretches at approximately 2900 cm^{-1} (Socrates, 2001). These are also present in the IR of *m*-xylene; however, the transmission decreased from around 90 % for *m*-xylene to approximately 70 % for the product. This suggests a higher number of C-H stretches in the product, which is to be expected. The other two distinct peaks at 846 and 705 cm^{-1} are typical of C-H out-of-plane bending stretches in 1,3,5-trisubstituted benzene (Mayo, Miller & Hannah, 2004).

The band at 769 cm^{-1} is indicative of a 1,3-disubstituted benzene (Mayo, Miller & Hannah, 2004) and can therefore be assigned to residual *m*-xylene that had not been successfully separated during the vacuum distillation or rotary evaporation process. However, the band increased from 80 % transmission to around 87 % transmission upon purification by rotary evaporation, confirming the loss of *m*-xylene. There is also a strong band at 1603 cm^{-1}, which can be assigned to C=C stretches in aromatic compounds (Socrates, 2001).

Interpretation of the mass spectrum also supports the formation of the expected monoalkylated product. It can be concluded that polyalkylation had not occurred, most likely due to the high ratio of *m*-xylene to *t*-butyl in the reagents.

A closer look at the GC-FID in Figure 12 allows the observation of 2-3 smaller peaks either side of the predominant product peak. GC-MS showed that the peak to the right at 12.79 minutes had a similar fragmentation pattern with the same molecular ion peak -- the peak at m/z 207 is most likely due to column bleed. This suggests a 1,2,3- or 1,2,4-trisubstituted isomer of *t*-butyl xylene. Another possibility, however, is *ipso* attack which would lead to a different isomer. In *ipso* attack, the alkyl cation attacks at the carbon already occupied with a methyl constituent. This could then lead to a [1,2] migration of the methyl group followed by proton loss. The likelihood of these isomers will be discussed later in the report.

Interestingly, GC-FID analysis showed a match of retention times for the peak at 8.71 minutes with *m*-xylene. However, the fragmentation pattern for this peak is not consistent with what should be expected. The large m/z of the molecular ion peak suggests polyalkylation may have occurred, however trialkylation would have yielded a product with a mass of 274 g mol^{-1}, which again is inconsistent with the data.

Table 5: Interpretation of the mass spectrum of the primary product of the Friedel-Crafts alkylation of *m*-xylene

m/z	Interpretation of peak	Structure of fragment
162	Molecular ion peak	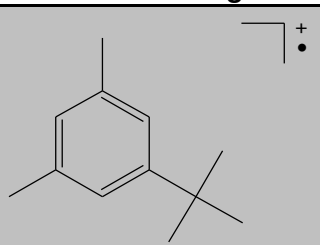
147	Base peak -- loss of a methyl group. Most abundant due to a high number of places where fragmentation could occur	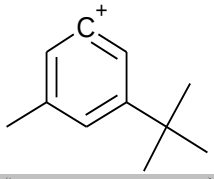
119	Potentially loss of three methyl groups, however this would lead to a fragment with m/z 117, so more complex rearrangements may have occurred	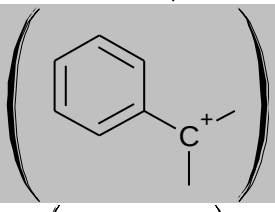
107	Again, potentially loss of the *t*-butyl group, however this fragment would have m/z of 105, so more complex rearrangement may have occurred	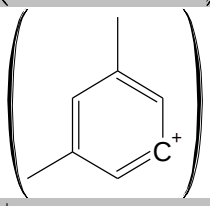
91	Benzyl carbocation, will undergo rearrangement to form the tropylium ion	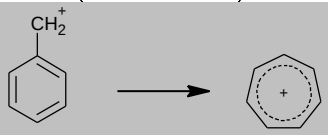
77	Phenylium ion	
65	Breakup of the phenylium ion or smaller fragments	

The ^{13}C and DEPT spectra show a low number of peaks for the molecule, which suggests a high level of symmetry. This suggests the product is either in the 1,3,5- or 1,2,3- configuration.

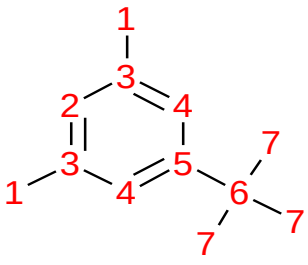

Figure 36: The labelling of carbon environments to allow assignment of peaks

Table 6: Interpretation of the 13C and DEPT spectra of the Friedel-Crafts alkylation product

Chemical Shift (ppm)	Environment	DEPT peak	Interpretation
151.2	5	Not present	The peak's absence on the DEPT spectra and high chemical shift suggest that this is an aryl quaternary carbon. This has been assigned to position 5 due to its low intensity.
138	3	Not present	The DEPT spectrum suggests that this peak is due to a quaternary carbon. Due to its high intensity, it has been assigned to carbon 3.
126	2	Upwards	Due to either a primary or tertiary carbon in the molecule, as indicated by the DEPT spectrum. A high chemical shift suggests an aromatic carbon. It has been assigned as 2 as its intensity is roughly half that of the other aryl primary carbon.
124	4	Upwards	Due to either a primary or tertiary carbon as indicated by the DEPT spectrum. It has been assigned to 4 due to its intensity being roughly double that of the other aryl primary carbon.
35	6	Not present	This small peak has been assigned to position 6 as it has a small intensity and the DEPT spectrum indicates it is a quaternary carbon. Its lower chemical shift suggests an aliphatic carbon.
27	7	Upwards	The large intensity is due to the fact there are three carbons in this magnetic environment as opposed to one. Its positive deviation on the DEPT spectrum suggests this is due to primary carbons, and again the low chemical shift is in accordance with it being an aliphatic carbon.
23	1	Upwards	As there are 2 carbons in this magnetic environment, the peak is quite high -- although not as high as position 7, which has 3 carbons. Again, it is a primary, aliphatic carbon due to its positive peak on the DEPT spectrum and low chemical shift.

The proton NMR (Figures 18 and 19) also show a high level of symmetry as there are only four significant peaks when integrated. The interpretation of this spectrum supports the IR evidence and allows the conclusion of the 1,3,5- isomer being former.

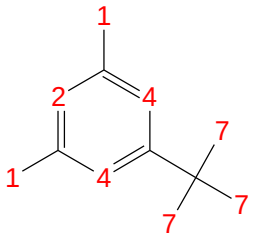

Figure 37: The labelling of proton environments to allow assignment of peaks

Table 7: The interpretation of the ^{1}H NMR spectrum for the product of the Friedel-Crafts alkylation

Chemical shift (ppm)	Integration	Multiplicity	Environment	Comments
1.30	9	Singlet	7	Methyl groups of the *t*-butyl group, high field
2.31	6	Singlet	1	Methyl groups attached to benzene, slightly lower field due to polarity of the benzene ring
6.82	1	Singlet	2	Low field suggests aryl protons. Due to integration, assigned to environment d
7.00	2	Singlet	4	Low field suggests aryl protons. Due to integration, assigned to environment c
7.24	0.09	Singlet	n/a	Most likely due some protons found in the deuturated chloroform solvent

Analysis of the Friedel-Crafts alkylation product confirms a 1,3,5-trisubstituted benzene, whilst gas chromatography has also shown the synthesis of isomers

Friedel-Crafts acylation

The yield for the acylation of *m*-xylene was higher than that for alkylation at 82 %. The purity of the product was also very high without a need for further purification -- using the areas of the peaks on the gas chromatogram, a purity of 98.6 % was calculated. The high yield is most likely due to the lack of purification as this is where significant losses were believed to have occurred for the alkylation.

The infrared spectrum of the product showed the characteristic C=O stretch at 1679 cm^{-1} which is in the range of an aromatic ketone. C-H stretches were also seen between 2874 and 2962 cm^{-1} although the transmittances of these are slightly higher than those in the alkylation product due to fewer C-H bonds present. The weak band at 891 cm^{-1} coupled with the strong band at 810 cm^{-1} suggests a 1,2,4- trisubstituted benzene (Mayo, Miller & Hannah, 2004).

Again, the MS data supports the formation of the expected product.

The smaller peak at 14.88 minutes showed a similar mass spectrum to the dominant peak; however, the peak at m/z 161 did not appear. This is believed to have been due to the 1,2,3- or 1,2,5-trisubstituted isomer. Although IR analysis would allow determination of the pattern of substitution, the extremely low concentration suggests

that any peaks concerning this cannot be confidently assigned due to a high transmittance.

The large number of peaks in the ^{13}C and DEPT spectra suggests a low level of symmetry, which is in accordance with the IR spectrum, as the only isomer with no symmetry is the 1,2,4- trisubstituted product. The spectra can therefore be interpreted as per figure 38.

Table 8: Interpretation of the mass spectrum for the principle product of the Friedel-Crafts acylation

m/z	Interpretation	Structure of fragment
176	Molecular ion peak	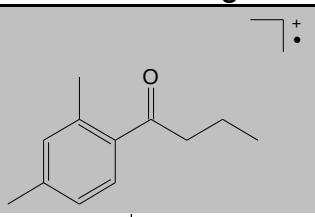
161	Loss of methyl group	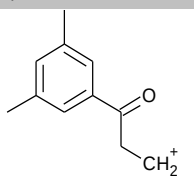
133	Base peak -- acylium ion. Most abundant fragment due to resonance stabilised structure	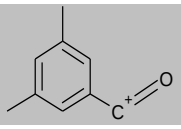
105	Could be several fragments: acylium ion, dimethyl phenylium ion or methyl benzyl carbocation.	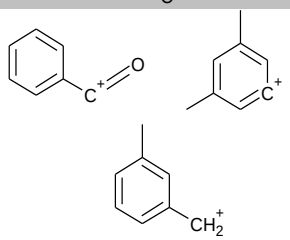
77	Phenylium ion	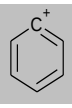
51	Breakup of the phenylium ion or smaller fragments	

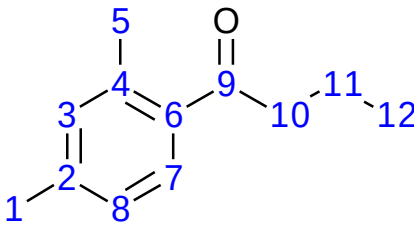

Figure 38: The labelling of the carbon environments to allow assignment of peaks for the acylation product

Table 9: The interpretation of the ^{13}C and DEPT spectra of the product of the Friedel-Crafts acylation of *m*-xylene

Peak (ppm)	Environment	DEPT peak	Interpretation
204.2	9	Not present	Carbonyl carbon. Lack of the peak on the DEPT spectrum indicates a quaternary carbon. High chemical shift suggests the carbon is close to an electronegative atom.
141.6, 138.5, 135.4	2, 4, 6	Not present	Due to the high chemical shift, these are most likely due to the aryl carbons where the substituents occur. The DEPT spectrum indicates that these are quaternary carbons. Cannot be assigned to specific peaks with any real confidence.
132.9, 129.0, 126.3	3, 8, 7	Upwards	Unsubstituted aryl carbons. High chemical shift suggests aromaticity whilst their positive deviations on the DEPT spectrum suggest they are either primary or tertiary.
77.40, 77.08, 76.77	n/a	Not present	Solvent peaks.
43.3	10	Downwards	Secondary carbon, due to the higher chemical shift this is most likely due to the CH_2 closest to the C=O.
21.5, 21.4	1, 5	Upwards	These peaks are most likely due to the 2 CH_3 groups in the 1, 4 positions. Proximity to each other indicates their very similar magnetic environment and their slightly higher chemical shift may be due to the aromatic ring.
18.4	11	Downwards	This is most likely due to the CH_2 group further away from the C=O bonds due to its lower chemical shift. Its peak on the DEPT spectra deviates downwards, indicating a secondary carbon.
13.9	12	Upwards	Assigned to the terminal CH_3 group on the acyl substituent. Its chemical shift is lower than those attached directly to the aromatic ring as the environment is less influenced by it.

Interpretation of the proton NMR spectrum drew the same conclusions about the structure of the product.

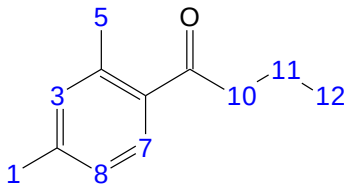

Figure 39: The labelling of the proton environments to allow assignment of peaks for the acylation product

Table 10: The interpretation of the ^{1}H proton NMR and assignment of the peaks to the proton environments for the acylation product (chemical shift range of 0 - 4 ppm)

Chemical shift (ppm)	Integration	Multiplicity	Environment	Comments
0.96	3	Triplet	12	Terminal methyl group on the acyl chain due to it being high field with an integration of 3.
1.70	2	Sextet	11	Due to the multiplicity of the peak, this must be assigned to environment 11.
2.32	3	Singlet	1	Due to the integration and multiplicity of this peak, assigned to environment 1 as 5 is closer to the oxygen, however this cannot be assigned with much confidence.
2.46	3	Singlet	5	As this peak is slightly lower field, it was assigned to environment 5 due to its proximity to the oxygen atom.
2.83	2	Triplet	10	This CH_2 group has a low field shift due to its proximity to the oxygen atom.

Table 11: The interpretation of the aromatic protons of the acylation product concerning the 1H proton NMR (chemical shift range of 6 - 8 ppm)

Chemical shift (ppm)	Integration	Multiplicity	Environment	Comments
7.24	0.19	Singlet	n/a	Most likely due to some residual protons in the deuturated chloroform solvent.
7.55	1	Doublet	7/8	Due to either 7 or 8. Chemical shift characteristic of an aromatic proton (low field) and splitting is consistent with one neighbouring proton.
7.03	2	Singlet/ Doublet	3 and 7/8	At first sight, multiplicity appears to be a singlet, however at high magnifications a doublet can be seen within. An

	integration of 2 suggests 2 aromatic protons, therefore the singlet can be attributed to 3 and the doublet can be attributed to either 7 or 8.

Comparison of alkyl and acyl products

Perhaps the most notable comparison between the alkyl and acyl products is the position of the substitution. The alkyl product formed in the 1,3,5- configuration whilst the acyl product formed in the 1,2,4- configuration. As has previously been discussed in the introduction, the pre-existing methyl groups are *ortho-para*- directing yet due to steric hindrance, the *para*- product dominates. Hence, one would expect to see substitution at these positions to yield a 1,2,3- and 1,2,4- configuration. This is due to the relative stabilities of the carbocation intermediates. In Figure 40, it can be seen that the carbocation intermediates involve structures with the positive charge being placed at positions 1,3- for the *para*- and *ortho*- attacks. The methyl groups at these positions are therefore able to stabilise this positive charge due to their electron-donating nature. However, the *meta*- attack intermediates do not allow the positive charge to be placed at these positions and hence no stabilisation of the carbocation can occur.

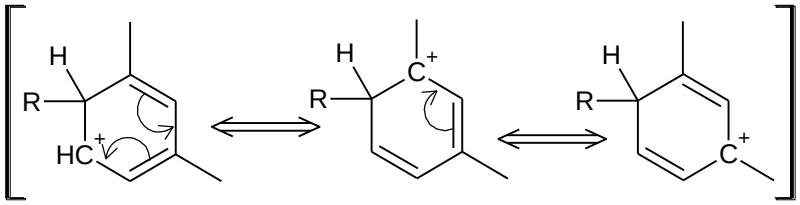

Para- attack intermediates

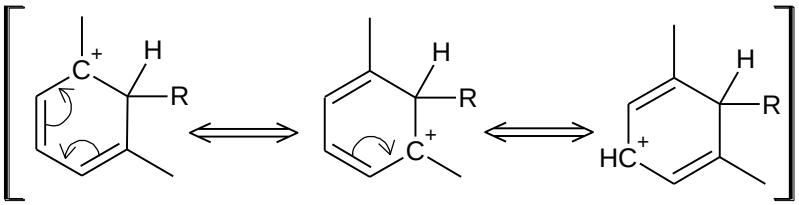

Ortho- attack intermediates

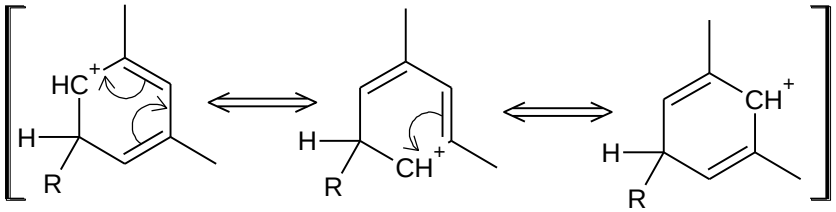

Meta- attack intermediates

Figure 40: The resonance structures of the intermediate carbocations in the acylation and alkylation of *m*-xylene

As has previously been mentioned, *ipso* attack followed by a [1,2] migratory methyl shift could also yield a second isomer -- a *t*-butylated *o*-xylene product. However steric hindrance at this position makes the attack unlikely.

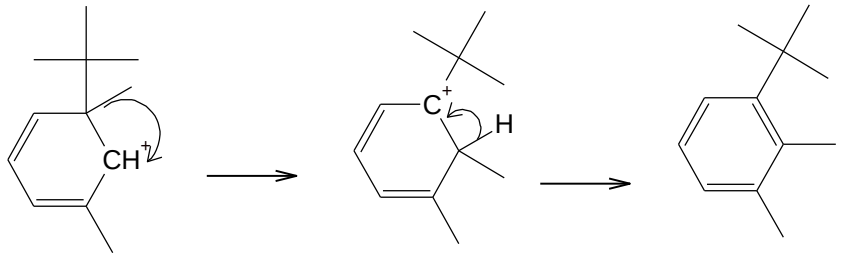

Figure 41: The [1,2] migratory shift for the methyl group subsequent to *ipso* attack

Whilst the product of the acylation of *m*-xylene was in accordance with predictions of *para*- attack, the alkylation occurred at the *meta*-position. This is in conflict with previous literature, whereby Ismail *et al.* (2008) studied the alkylation of *m*-xylene by *t*-butyl chloride and concluded a 1,2,3- and 1,2,4- trisubstituted benzene product .

There are several reasons why the alkylation could have taken place at the *meta*-position. Firstly, the *t*-butyl substituent is branched, whereas the butyryl group is straight chain. The branched aspect of the substituent adds greater steric hindrance in the 1,2,3- and 1,2,4- trisubstituted products, which may have overcome the increased stability of the intermediates. Furthermore, despite the intermediates being at a lower energy due to high stabilisation, the 1,2,4- product will have a higher energy than the 1,3,5- product due to the steric factor (see Figure 43).

t-alkylation is also one of the most important reversible aromatic substitution reactions. Bearing this is in mind, it is possible to have de-*t*-alkylation of the product and then re-attack of the *t*-butyl cation (Bruckner, 2001). If this were the case, the *t*-butyl cation is bound to the aromatic nucleus in such a way that is dictated by thermodynamic control (Bruckner, 2001). For example, 1,2,4-tri-*t*-butylbenzene can be isomerised to give 1,3,5-tri-*t*-butylbenzene (Bruckner, 2001). This would suggest that the 1,3,5- positions are favoured due to the steric hindrance in place. A question that could reason the difference in products is whether the reaction is kinetically or thermodynamically controlled.

It can be seen in Figure 42 that product C is more thermodynamically stable than product B as it has lower ΔG, however product B will form faster due to the lower $\Delta G^{\neq}$. When neither reaction is reversible, product B will be formed in a greater quantity as the reaction is faster (March, 1992). Therefore, the product is deemed to be kinetically controlled. However, if reversibility of the reactions A → B and A → C is possible then the predominant product will be C, so long as the reaction is allowed to reach equilibrium (March, 1992). In this scenario, B will be formed first due to its faster kinetics, however it will then revert to product C due to its higher stability. In this case, the reaction is said to be thermodynamically controlled (March, 1992).

It is stated by March (1992) that pre-existing groups will direct predominantly but not exclusively. He also states that the orientation and reactivity of these groups can be explained by the resonance and field effects on the stability of the intermediate carbocation (see Figure 40) (March, 1992). This is due to the reactions usually being kinetically, not thermodynamically controlled.

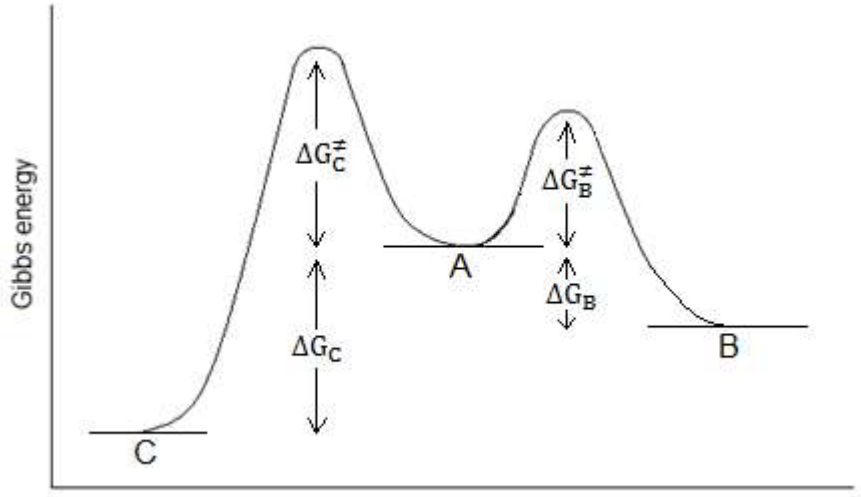

Figure 42: An energy diagram illustrating kinetic vs. thermodynamic control. The starting compound A can react to give either B or C (March, 1992)

As many reactions are irreversible or stopped before the equilibrium position is reached, it is assumed that the intermediates formed are based on the activation energy required to form them as opposed to the thermodynamic stability of the products. Hence, it is possible that, due to the reversibility of *t*-butylation, the intermediates formed are instead dependant on the thermodynamic stability of the products (March, 1992). For example, the sulfonation of naphthalene at lower temperatures favours the α-isomer as the reaction does not reach equilibrium, however at higher temperatures where the reaction can equilibrate the β isomer predominates as due to steric interactions this is the thermodynamically favourable product (March, 1992).

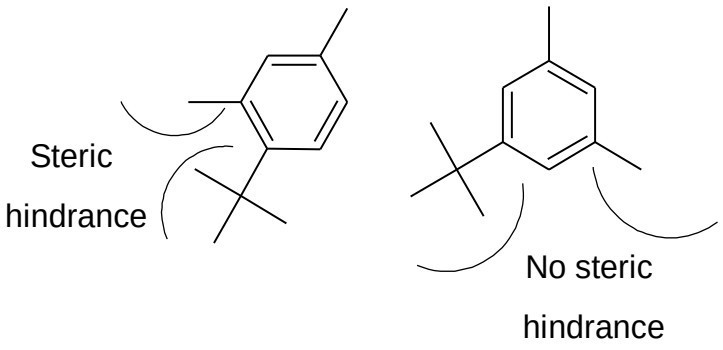

Figure 43: A graphical representation of the steric hindrance, which takes place between neighbouring substituents and how this can be minimised through isomerisation

Figure 43 shows how attack at the *para/ortho* position increases steric hindrance with regards to the stability of the products. Relating this to the energy diagram in Figure 42, the starting product A would be *m*-xylene and products B and C would be the 1,2,4- and 1,3,5 tri-substituted products respectively.

The concept of kinetic control vs. thermodynamic control is much discussed in literature. Whilst it was initially reported that the Friedel-Crafts acylation reaction differed from the alkylation in that it was almost entirely irreversible (Olah, 1973), evidence of the reversibility of Friedel-Crafts acylations are becoming more apparent.

It is reported that Friedel-Crafts acylations can be adjusted to give a kinetically controlled ketone or a thermodynamically controlled ketone (Mala'bi, Pogodin & Agranat, 2011). Thermodynamic control has been associated with acyl rearrangements and reversibility of reactions, however whether they are thermodynamically or kinetically controlled is still an open question (Mala'bi, Pogodin & Agranat, 2011).

Concerning the current work, the products gained from the acylation and alkylation reactions suggests that Friedel-Crafts acylation of *m*-xylene is an irreversible process and therefore the product is kinetically controlled. Alkylation, on the other hand, can be concluded to be a reversible reaction, which allows the product to be thermodynamically controlled. Therefore, the more stable 1,3,5- product was formed.

The mechanism of Friedel-Crafts acylation

The first step in the mechanism is the creation of the electrophile via complexation of the acyl chloride with the aluminium chloride.

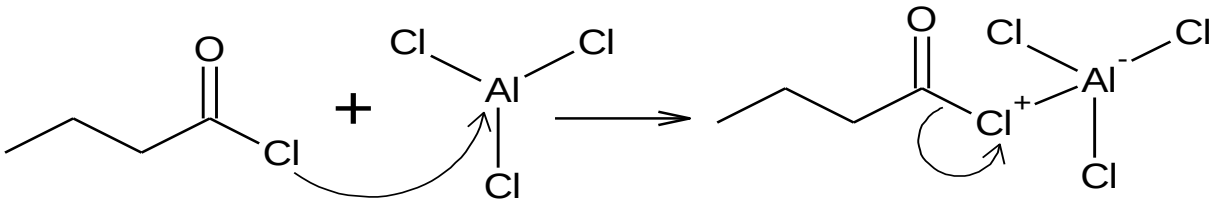

Figure 44: The complexation of butyryl chloride with aluminium chloride

Although this is generally the preferred representation in literature, in fact, infrared spectra of acyl chloride/aluminium chloride mixtures have revealed free acylium ions as well as 1:1 and 1:2 complexes. X-ray studies have also confirmed that the 1:1 complex is coordinated via the oxygen (Jones, 1984).

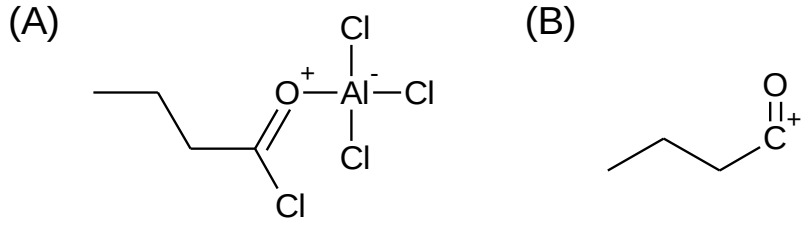

Figure 45: (A) the 1:1 adduct and (B) the free acylium ions, which can react with the xylene (Jones, 1984)

Figure 45 shows two of the components in the acyl chloride/aluminium chloride mixture, where the 2:1 complex may form by further complexation at the chlorine (Jones, 1984).

An X-ray study, which looked at the acylation mechanism concerning different Lewis acids, showed that coordination at the carbonyl-oxygen centre of the acid chloride was preferential (Davlieva *et al*., 2005). The X-ray structural parameters showed significant elongation of the carbonyl bond and shortening of the C-Cl. These indicate increased electron deficiency induced at the carbonyl centre by Lewis acid coordination which is compensated by the π-electron donation from chlorine,

strengthening the C-Cl bond (Davlieva *et al.*, 2005). There is no evidence for a coordinated complex between the Lewis acid and the chlorine centre suggesting this adduct is not mechanistically significant (Davlieva *et al.*, 2005). It is therefore theorised that the formation of the acylium ion involves the rearrangement of the 1:1 complex (Figure 46).

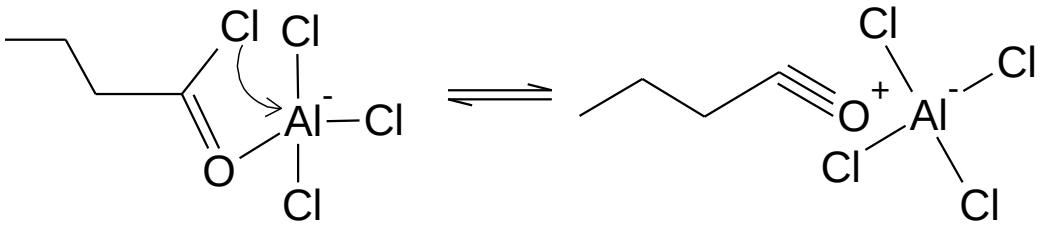

Figure 46: The intramolecular rearrangement of the 1:1 Lewis acid complex (Davlieva *et al.*, 2005)

Figure 47 then displays the formation of the σ complex with the acylium ion, although either of the displayed electrophiles in Figure 45 may be involved in the attack. This is dependent on the nature of the solvent, acyl chloride and substrate (Jones, 1984).

The σ complex intermediate is commonly called the Wheland intermediate and the transition state has the positive charge shared between the electrophile and the aromatic ring (Jones, 1984). Olah *et al.*, however, interprets two intermediates with two transition states -- a π complex and a σ complex (Olah, Kuhn & Flood, 1962). He suggested the π complex existed as an electrophilic ion being associated with a benzene π system, but without being specifically bonded to a particular carbon atom (Olah, 1963).

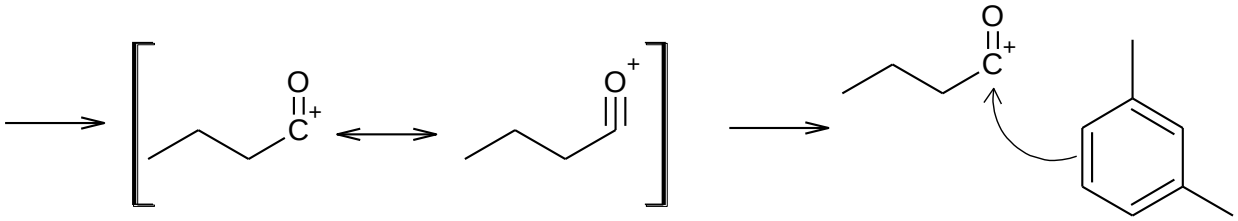

Figure 47: The formation of the σ complex by electrophilic aromatic substitution

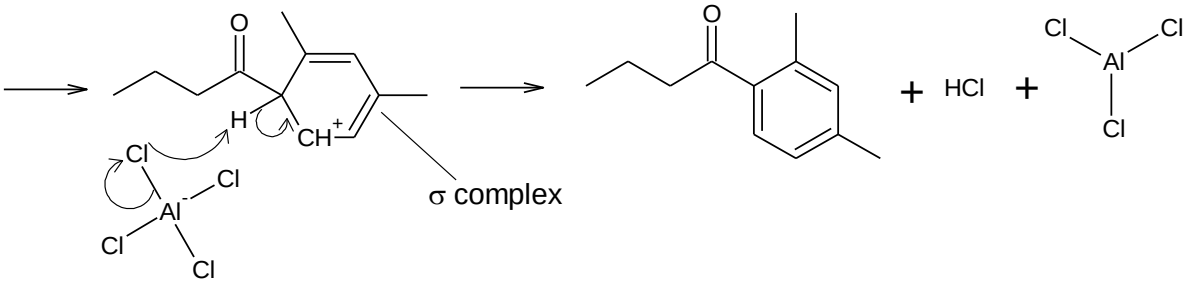

Figure 48: The de-protonation step leading to the re-aromatisation

Figure 49 shows an energy diagram for the reaction with the π and σ intermediate complexes included.

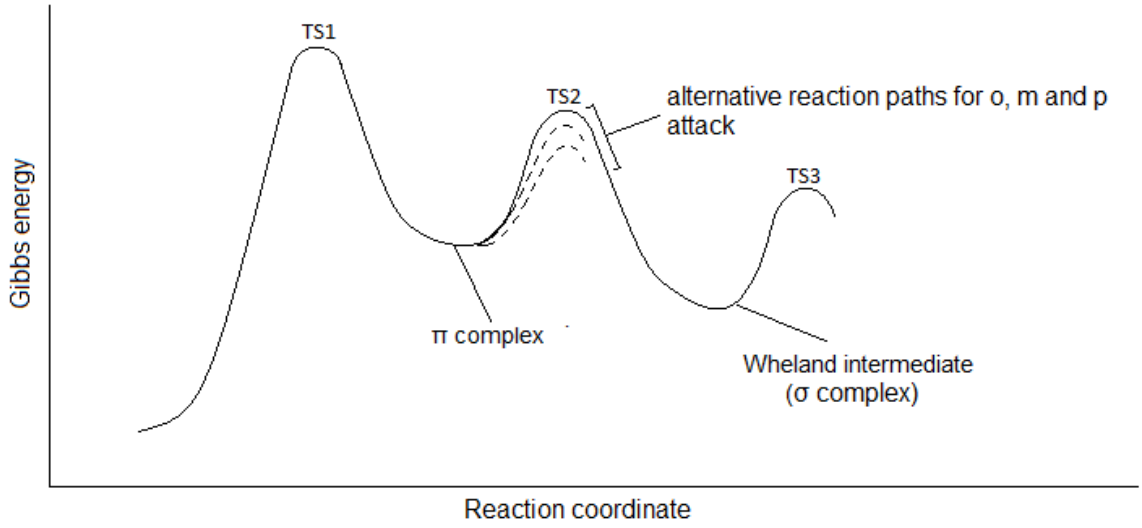

Figure 49: The rate limiting π complex formation showing the energy of the transition states (where TS3 is the loss of a proton) (Jones, 1984)

Concerning the mechanism of acylation, there is significant discussion about whether the π or σ complex is the rate-determining step. Although some literature has stated the de-protonation step to be at least partially rate determining, a study by Zhu & Meyer (2011) suggested that de-protonation is not rate limiting and can be excluded as the product-determining step. This is in accordance with Davlieva *et al.* (2005) who state that rapid proton loss occurs from the Wheland intermediate. A more detailed account of the deprotonation step can be seen in a later section, where it is compared to deprotonation in alkylation.

The results of the study by Zhu & Meyer (2011) presented suggest a rate- and product-limiting σ complex formation in the Friedel-Crafts acylation of xylene.

The mechanism for Friedel-Crafts alkylation

The literature available on the mechanism for Friedel-Crafts alkylation is not as vast as it is for acylation due to the reactions' associated problems (polyalkylation and cation isomerism).

The mechanism as defined by Clayden *et al.* (2012) can be seen in Figure 50.

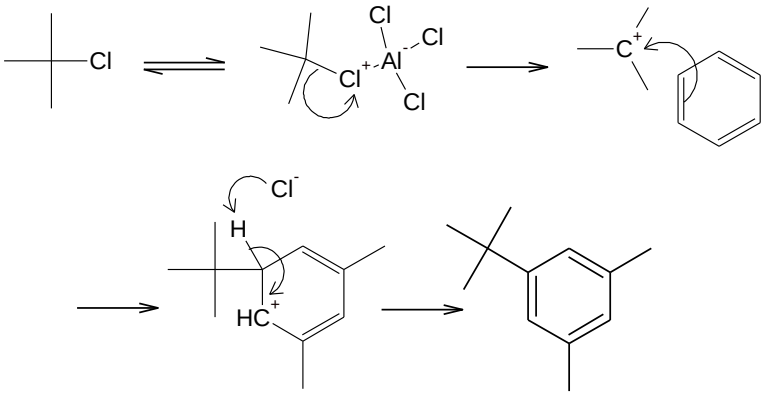

Figure 50: The mechanism for the *t*-butylation of *m*-xylene via Friedel-Crafts alkylation (Clayden, Greeves & Warren, 2012)

The first step involves bond formation between RX and $AlCl_3$ to form a cation, which then forms a σ complex (the Wheland intermediate). No rearrangement of the carbocation is seen as, being a tertiary carbocation it is already in its most stable form.

The transition states in this mechanism, however, have been oversimplified and other literature shows a far better insight. Although direct evidence from IR and NMR spectra show that the *t*-butyl cation is quantitatively formed when *t*-butyl chloride interacts with $AlCl_3$, the methylation of toluene by methyl bromide and methyl iodide shows different *ortho/para/meta* ratios. Hence, it is suggested that instead that the carbocation exists as either a complex or a tight ion pair with $AlCl_4$, similar to the acylation mechanism (March, 1992).

A series of intermediates have been isolated and studied via density functional theory calculations, which show the complexation of the catalyst to the cation (Yamabe & Yamazaki, 2009). Interestingly, it is stated that $AlCl_3$ exists as a dimer in non-polar solvents (such as *m*-xylene and DCM) and hence all of the intermediates formed include an Al_2Cl_6 bridge (Yamabe & Yamazaki, 2009).

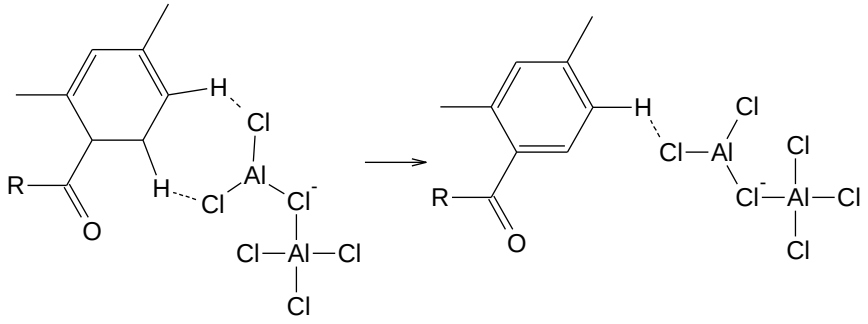

Figure 51: Deprotonation of the Wheland intermediate in a Friedel-Crafts acylation

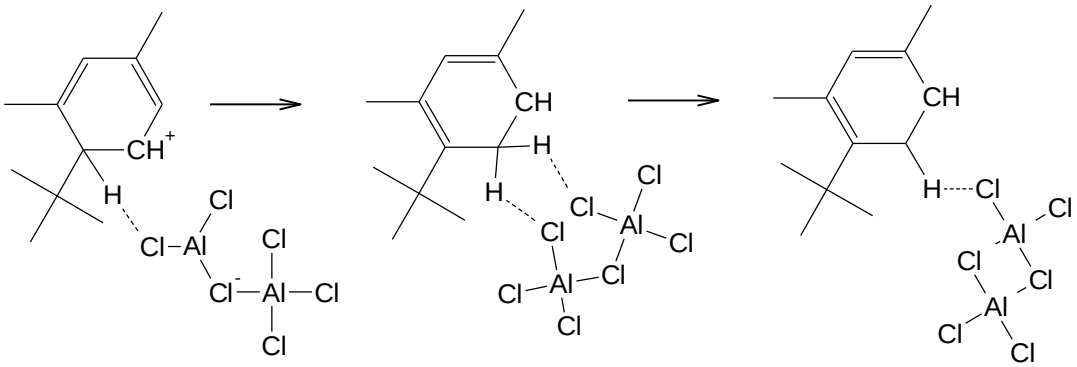

Figure 52: [1,2] H-shift in the Wheland intermediate leading to an *ortho*-protonated species with subsequent deprotonation (Yamabe & Yamazaki, 2009)

Figures 51 and 52 show the difference in the deprotonation step between the alkylation and acylation mechanisms. As can be seen, whilst deprotonation of the Wheland intermediate in the acylation leads to a complex between the acylated xylene and H-Cl-Al_2Cl_6, the alkylation intermediate first undergoes a migratory [1,2] H-shift to yield an *otho*-protonated species (Yamabe & Yamazaki, 2009). This intermediate then undergoes deprotonation to yield the final product, recovering the Al_2Cl_6 bridge (Yamabe & Yamazaki, 2009). The regeneration of this catalyst is concordant with experimental findings, where only a catalytic amount of Lewis-Acid

was used for the alkylation, whilst the acylation reaction required a higher mass. This is echoed by Clayden *et al.* (2012) who states that acylation requires just over one equivalent per carbonyl group.

Grignard products

The yield for the reaction using ethyl bromide was significantly low at just 1.2 %, whilst the yield using propyl bromide was high at 72 %. Despite this, evidence of an alcohol being formed can be seen in the IR spectrum with a broad peak at around 3500 cm^{-1}. The chromatogram also showed evidence of a new product being formed with a peak at 16.55 minutes. However, the peak area of this was relatively low and hence the product was deemed to have a low purity at just 38.8 %. GC-MS analysis confirmed the synthesis of a tertiary alcohol with the addition of an ethyl group.

Table 12: Interpretation of the mass spectrum of the Grignard product with ethyl bromide

m/z	Interpretation of peak	Structure of fragment
188	Dehydration -- loss of H_2O	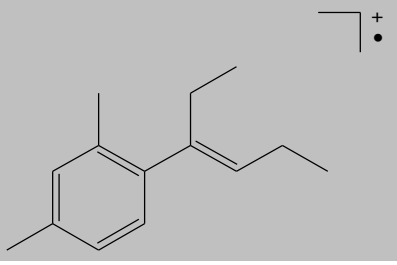
177	Base peak -- loss of the ethyl group. Stabilised by resonance	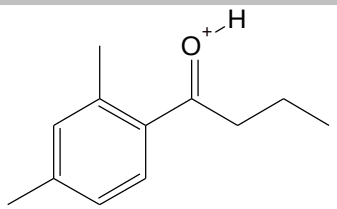
173	Loss of a methyl group from the dehydration group	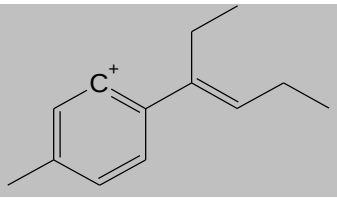
163	Loss of the propyl group. Stabilised by resonance.	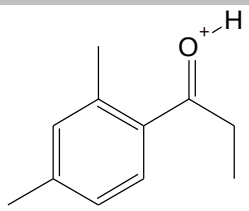
159	Loss of alcohol and ethyl group	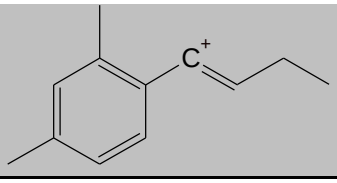

Table 13: Further interpretation of the mass spectrum of the Grignard product with ethyl bromide

m/z	Interpretation of peak	Structure of fragment
145	Loss of the propyl group from the dehydration product	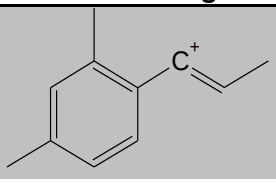
115	Loss of the propyl group and loss of the two xylene methyl groups	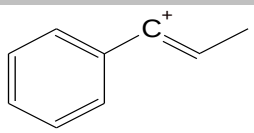
105	Dimethyl phenyl carbocation	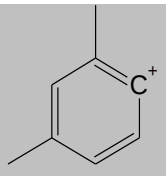
91	Benzyl carbocation / tropylium ion	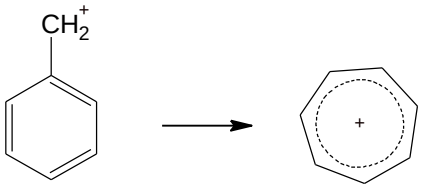
77	Phenylium ion	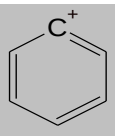
65, 51	Break up of phenylium ion	

The IR of the product using propyl bromide also displayed a broad alcohol peak at 3500 cm^{-1} (Socrates, 2001), however the chromatogram showed impurities of the starting ketone and another reagent (15.46 and 13.90 minutes respectively). This is supported by the IR spectrum, which shows a significant carbonyl peak at 1679 cm^{-1}. The product peak appears at 17.01 minutes, and indicated a purity of 36.4 %. Again, GC-MS allowed the confirmation of a successful synthesis.

Table 14: Interpretation of the mass spectrum of the Grignard product with propyl bromide

m/z	Interpretation of peak	Structure of fragment
202	Dehydration of alcohol -- loss of H_2O	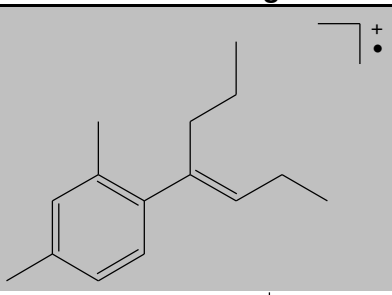
187	Dehydration followed by loss of a methyl group	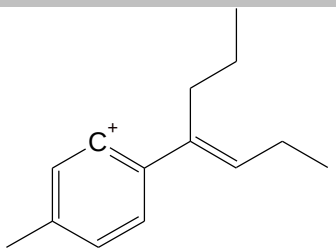
177	Loss of a propyl group	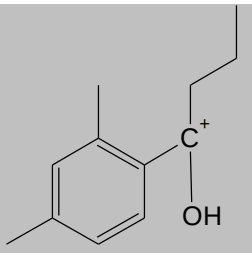
159	Dehydration followed by a loss of propyl group	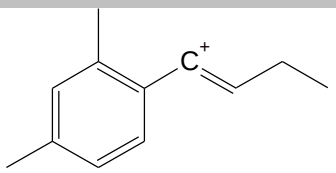
145	Dehydration followed by loss of a propyl group then loss of a methyl group	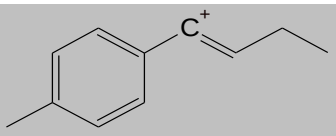
133	Loss of two propyl groups	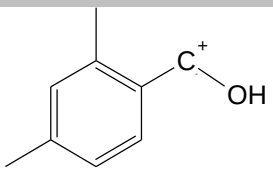
119	Loss of two propyl groups and a methyl group	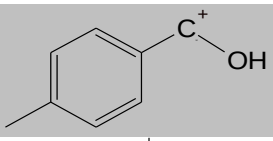
105	Dimethyl phenylium ion	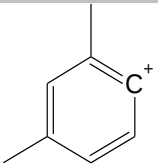

Table 15: Interpretation of the smaller fragments in the mass spectrum of the Grignard product with propyl bromide

m/z	Interpretation of peak	Structure of fragment
91	Benzyl carbocation	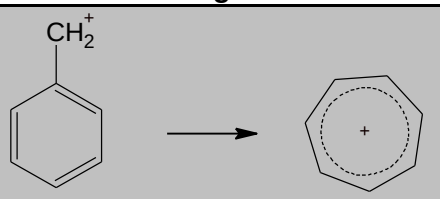
77	Phenylium ion	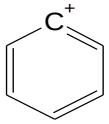
71 and 55	Break up of phenylium ion and smaller fragments	

The GC-MS chromatogram showed a number of peaks, many of which produce the same mass spectrum by GC-MS. For the alcohol obtained using ethyl bromide, 5 peaks on the GC-MS produce a similar fragmentation pattern -- retention times 12.57, 11.18, 11.13, 10.45 and 10.33 min. The molecular-ion m/z for the most abundant peak (12.57 min.) is 189, whilst for the remaining four peaks it is 188. This suggests that the alcohol peak is at 12.57 min. and that the other peaks are subsequent dehydration of the alcohol product. Due to an issue with the oven of the GC-FID instrument, all chromatograms exhibited a positive retention time shift. Hence, retention times of the GC-MS chromatograms are not consistent with the GC-FID chromatograms. However, logic suggests the GC-MS predominant product peak at 12.57 min. appears at 17.01 min. with the GC-FID.

Dehydration of an alcohol gives rise to an alkene, which allows geometric isomers to occur -- E/Z isomerism. The reduction of the carbonyl group could lead to formation of a π bond on either the propyl or the ethyl chain (see Figure 53). On either chain, E/Z isomerism can occur, leading to four possible isomers. The mass spectra suggest that these isomers can be separated by gas chromatography.

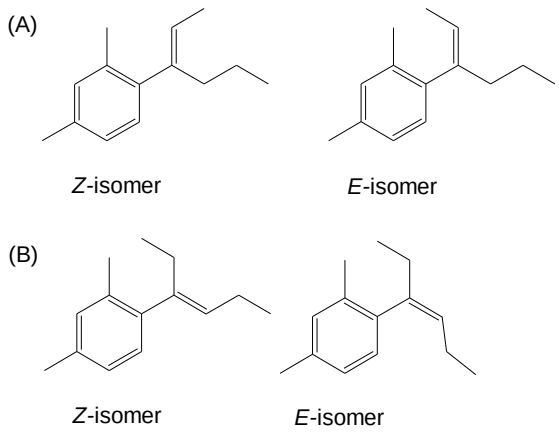

Figure 53: The E/Z isomers exhibited from the dehydration of the alcohol. (A) shows the π bond on the ethyl group. (B) shows the π bond placed on the propyl group.

Conversely, for the reaction with propyl bromide, the subsequent alcohol has two identical propyl groups attached. Therefore, the π bond can only be placed in one position. This means only two isomers are possible. The GC-MS confirms this, as only three peaks show similar fragmentation patterns -- 13.50, 12.15 and 11.39 min. The most abundant peak is at 13.50, with a molecular-ion mass of 202. The main difference in these three mass spectra is the bass peak -- m/z of 177 for the peak at 13.50 and an m/z of 159 for the other two. This suggests that the alcohol peak is indeed at 13.50 min. due to the resonance stabilisation of the fragment, which involves the alcohol group. The other two smaller peaks are again, E/Z isomerism of the dehydration product.

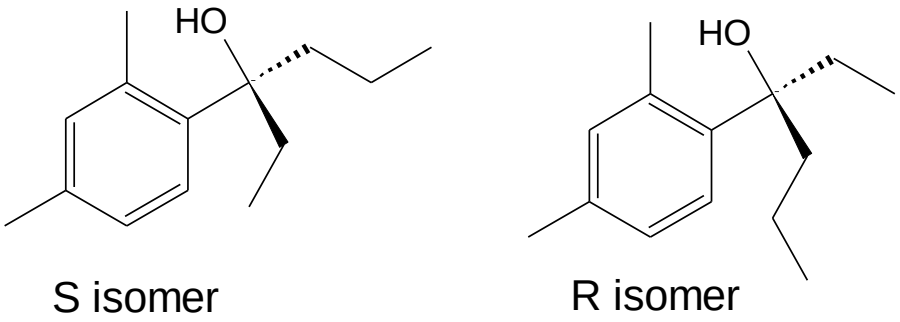

Figure 54: The two enantiomers one could produce from the *para*-substituted species

Another important aspect when reducing the carbonyl group is R/S isomerism. Figure 54 shows the enantiomers synthesised by introducing chirality to the original carbonyl carbon. R/S isomerism, however, would only be relevant to the synthesis using ethyl bromide due to the pre-existing propyl group. The GC-MS technique used was not selective enough to separate these enantiomers, which is challenging due to their identical physical properties such as boiling point and solubility. As most stationary phases are achiral, enantiomeric species have the same retention times and co-elution occurs (Robards, Haddad & Jackson, 1994).

The most common separation method for enantiomers is the use of a chiral capillary column whereby the stationary phase is manufactured to be chiral (Robards, Haddad & Jackson, 1994). Another potential route would be to derivatize the sample components with an optically active chiral reagent -- this would produce a pair of diastereoisomers that have different physical properties and could therefore be resolved on a typical achiral column (Robards, Haddad & Jackson, 1994). However, for practical reasons the use of a chiral capillary column is usually preferred (Robards, Haddad & Jackson, 1994).

In order to ascertain the reason for the poor yield using ethyl bromide, the mechanism for the Grignard reaction can be considered. The Grignard reaction is based on three steps -- the formation of the Grignard reagent RMgX, the reaction with the ketone and then a work-up stage. Therefore, the reason for the low yield of the reaction with ethyl bromide could have occurred at either of these stages.

The formation of the Grignard reagent is classed as a formal oxidative addition, and therefore in order to gauge the efficiency of this step one can look at the reduction potentials of RX. In order for the formation of the reagent to be thermodynamically

achievable, ΔE must be positive. The reduction potential of Mg^{2+} to Mg is -2.375 V (Silverman & Rakita, 1996). The reduction potential of ethyl bromide in DMF against a reference electrode of saturated calomel electrode (SCE) is -2.17 and of propyl bromide with the same solvent and reference electrode is -2.22 (Silverman & Rakita, 1996). Therefore, one would expect a moderate reactivity for both, and in fact would expect a greater reactivity for ethyl bromide. Formation of the Grignard reagent was concluded to have been successful from observations as the solution turned to a dark grey colour. However, this may have occurred without initiation if the agitation was strong enough to shear the magnesium.

Other problems that can occur at this stage include incomplete drying and presence of free oxygen. A water content of above 0.02 wt% leads to an improper initiation (Silverman & Rakita, 1996). Whilst initially this could be considered problematic as the magnesium turnings were not dried prior to the reaction for the ethyl bromide reaction, it is stated that water content leads to a sudden initiation after all of the RX has been added which results in the reaction contents being spewed into the atmosphere (Silverman & Rakita, 1996). This did not occur and it can therefore be concluded that the reason for the low yield was most likely not caused by this initial step.

It can be seen from the GC-MS results that an alcohol did form so reaction of the reagent with the ketone and work up was deemed successful. It is possible that the low yield could be due to significant losses in the drying step of the method. After potassium carbonate was added, only a small amount of crude product was able to filter through -- just 0.21 g. It was concluded this was due to too much potassium carbonate being added to the solution, and therefore for the second reaction a far smaller amount was added. This led to a much higher yield, although the purity of the product was still low.

Due to a lack of time, purification of the product was not performed. However, the alcohol could be separated from the ketone either through column chromatography or through vacuum distillation.

Further research

The conclusions of this project allow the possibility of many routes to be taken for further research.

Firstly, the comparison of Friedel-Crafts alkylation with Friedel-Crafts acylation could be better investigated by performing each at different temperatures and comparing the configuration of the products at each step. It would be interesting to see whether the 1,3,5-trisubstituted benzene is only formed at higher temperatures due to the reaction reaching equilibrium, or whether one could form the 1,2,4-trisubstituted benzene via this route by lowering the temperature. Whilst it is possible that in fact the 1,2,4-trisubstituted benzene does not form at all due to the steric factor being too high, this cannot be ruled out at this stage of investigation.

Secondly, one could perform the Friedel-Crafts acylation with a branched acyl chloride in order to ascertain whether with a bulkier acyl chloride, the 1,3,5-trisubstituted product would also be formed. This could lead to conclusions concerning the reversibility of the Friedel-Crafts acylation.

Concerning the Grignard reactions, the dehydration and hydrogenation experiments were not carried out due to a lack of time. By carrying these out to completion, a look at yields would allow the comparison of alkylation and acylation as a route to the synthesis of alkyl xylenes.

Conclusion

The Friedel-Crafts alkylation and acylation both proceeded successfully to give tri-substituted benzenes, although the positions of substitutions differed. It was concluded after spectral analysis that the major product of the alkylation was a 1,3,5-trisubstituted benzene whilst the major product of the acylation was a 1,2,4-trisubstituted benzene.

These results suggest that although methyl groups are *ortho*- and *para*- directing, steric hindrance will also have a large effect on the product formed. Furthermore, whilst literature is in agreement that the product will depend largely on the stability of the intermediates and transition states, the product of the alkylation depended predominantly on the thermodynamic stability of the product itself. This was deemed to be due to the reversibility of the alkylation reaction which allowed the predominant product to be thermodynamically controlled. In contrast, the product of the acylation reaction was deemed to be kinetically controlled due to the irreversibility of the reaction. It is suggested that although the 1,2,4-alkyl xylene was predominantly formed first due to fast kinetics, this product then reverted to the 1,3,5-alkyl xylene due to its greater thermodynamic stability.

The Grignard syntheses were deemed successful as GC-MS and IR data showed the expected tertiary alcohols to be formed. The low yield of the reaction with ethyl bromide was deemed to be due to the drying step where too much potassium carbonate was added. This led to a low crude yield as well as a low purified yield. The yield of the reaction with propyl bromide was far higher when less potassium bromide was added. Although the GC-FID spectra showed a low purity for both, it was concluded that purification could be carried out by either column chromatography or vacuum distillation.

Concerning the efficiency of the reactions, acylation gave a higher initial purity and did not require any further purification, whilst the alkylation product did. Furthermore, the high excess of *m*-xylene required for the alkylation reaction to ensure monoalkylation may not be viable on an industrial scale and would have further cost implications.

Further research was suggested to investigate the positions of substitution for the acylation and alkylation Friedel-Crafts reactions at similar and varying conditions. Different reagents could also be used to investigate the steric effects of these reactions. It was suggested that purification and dehydration/hydrogenation of the alcohols could lead to comparable alkyl-xylenes.

References

Bruckner, R. (2001) *Advanced Organic Chemistry Reaction Mechanisms.* Burlington : Elsevier Science.

Chao, K. J. & Leu, L. J. (1989) Conversion of toluent and trimetrylbenzene over NAHY zeolites. *Zeolites*, 9 (3). pp 193-196.

Clayden, J., Greeves, N. & Warren, S. G. (2012) *Organic chemistry.* 2nd ed. / Jonathan Clayden, Nick Greeves, Stuart Warren. edn. Oxford: Oxford University Press.

Davlieva, M. G., Lindeman, S. V., Neretin, I. S. & Kochi, J. K. (2005) Isolation, X- ray structures, and electronic spectra of reactive intermediates in Friedel- Crafts acylations. *The Journal of Organic Chemistry*, 70 (10). pp 4013.

Hattori, K., Sajiki, H. & Hirota, K. (2001) Chemoselective control of hydrogenation among aromatic carbonyl and benzyl alcohol derivatives using Pd/C(en) catalyst. *Tetrahedron*, 57 (23). pp 4817-4824.

Ismail, M., Saha, M., Siddiky, M. N. A., Alam, M. Z. & Sharif, N. (2008) Reaction of xylenes with tert.-butylchloride in presence of anhydrous aluminium chloride. *Journal of Scientific & Industrial Research*, 67 (5). pp 371-373.

Jin, W. J., Li, T., Zhao, K. & Zhao, H. (2013) Monitoring the reaction between $AlCl_3$ and o-xylene by using terahertz spectroscopy. *Chinese Physics B*, 22 (11). pp 3.

Jones, R. A. Y. (1984) *Physical and mechanistic organic chemistry.* 2nd ed. edn. Cambridge : Cambridge University Press.

Juganaru, T., Ionescu, C., Bombos, D., Bombos, M. & Matei, V. (2007) Study of hydrogenation process of some aromatic hydrocarbons on Zn-H-ZSM-5 catalytic support. *Revista De Chimie*, 58 (10). pp 983-987.

Kaneko, M., Hayashi, R. & Cook, G. R. (2007) Intermolecular Friedel-Crafts reaction catalyzed by $InCl_3$. *Tetrahedron Letters*, 48 (40). pp 7085-7087.

Kim, J. C., Cho, K. & Ryoo, R. (2014) High catalytic performance of surfactant-directed nanocrystalline zeolites for liquid-phase Friedel-Crafts alkylation of benzene due to external surfaces. *Applied Catalysis a-General*, 470 pp 420-426.

Mala'bi, T., Pogodin, S. & Agranat, I. (2011) Kinetic control wins out over thermodynamic control in Friedel-Crafts acyl rearrangements. *Tetrahedron Letters*, 52 (16). pp 1854-1857.

March, J. (1992) *Advanced organic chemistry : reactions, mechanisms, and structure.* 4th ed. edn. Wiley.

Mayo, D. W., Miller, F. A. & Hannah, R. W. (2004) *Course notes on the interpretation of infrared and Raman spectra.* New York ; Wiley.

Odochian, L., Soldea, C., Paius, C., Mocanu, A. M. & Moldoveanu, C. (2010) Kinetic study on competitive alkylation of an arene mixture coming from the petrochemical industry. *Revista De Chimie*, 61 (3). pp 316-321.

Olah, G. A. (1963) *Friedel-Crafts and related reactions: General aspects.* New York: Interscience (Wiley).

Olah, G. A. (1973) *Friedel-Crafts chemistry.* New York ; London: Wiley.

Olah, G. A., Kuhn, S. J. & Flood, S. H. (1962) Aromatic Substitution. X.1 The $AlCl_3 \cdot CH_3NO_2$-catalyzed benzylation of benzene and n-alkylbenzenes with benzyl chloride in nitromethane solution. *Journal of the American Chemical Society*, 84 (9). pp 1688-1695.

Patrick, G. L. (2000) *Instant notes in organic chemistry.* Oxford : Bios Scientific.

Robards, K., Haddad, P. R. & Jackson, P. E. (1994) *Principles and practice of modern chromatographic methods.* London: Academic.

Rylander, P. (1979) *Catalytic hydrogenation in organic syntheses.* New York : Academic.

Silverman, G. S. & Rakita, P. E. (1996) *Handbook of Grignard reagents.* New York : Marcel Dekker.

Socrates, G. (2001) *Infrared and Raman characteristic group frequencies : tables and charts.* 3rd ed. edn. Chichester: Wiley.

Tan, W., Liu, M., Zhao, Y., Hou, K. K., Wu, H. Y., Zhang, A. F., Liu, H., Wang, Y. R., Song, C. S. & Guo, X. W. (2014) *Para*-selective methylation of toluene with methanol over nano-sized ZSM-5 catalysts: Synergistic effects of surface modifications with SiO2, P2O5 and MgO. *Microporous and Mesoporous Materials*, 196 pp 18-30.

Toch, K., Thybaut, J. W., Vandegehuchte, B. D., Narasimhan, C. S. L., Domokos, L. & Marin, G. B. (2012) A Single-Event Micro Kinetic model for "ethylbenzene dealkylation/xylene isomerization" on Pt/H-ZSM-5 zeolite catalyst. *Applied Catalysis a-General*, 425 pp 130-144.

Wang, T., Tang, F. M. & Wu, Y. F. (2011) A combined EPR and DFT study of the overcrowded aromatic radical cations from Friedel-Crafts alkylation reactions. *Journal of Molecular Structure*, 1002 (1-3). pp 128-134.

Xue, B., Zhang, G., Liu, N., Xu, J., Shen, Q. & Li, Y. (2014) Highly selective synthesis of *para*-diethylbenzene by alkylation of ethylbenzene with diethyl carbonate over boron oxide modified HZSM-5. *Journal of Molecular Catalysis a-Chemical*, 395 pp 384-391.

Yamabe, S. & Yamazaki, S. (2009) A remarkable difference in the deprotonation steps of the Friedel–Crafts acylation and alkylation reactions. *Journal of Physical Organic Chemistry*, 22 (11). pp 1094-1103.

Zhang, Y.-Y., Li, Y.-F., Chen, L., Au, C.-T. & Yin, S.-F. (2014) A new catalytic process for the synthesis of *para*-xylene through benzene methylation with CH_3Br'. *Catalysis Communications*, 54 pp 6-10.

Zhu, H. & Meyer, M. P. (2011) Cationic intermediates in Friedel-Crafts acylation: structural information from theory and experiment. *Chemical Communications*, 47 (1). pp 409-411.